Self-Assembly

*The **spontaneous and reversible** association of molecular species to form larger, more complex supramolecular entities according to the **intrinsic information** contained in the components.*

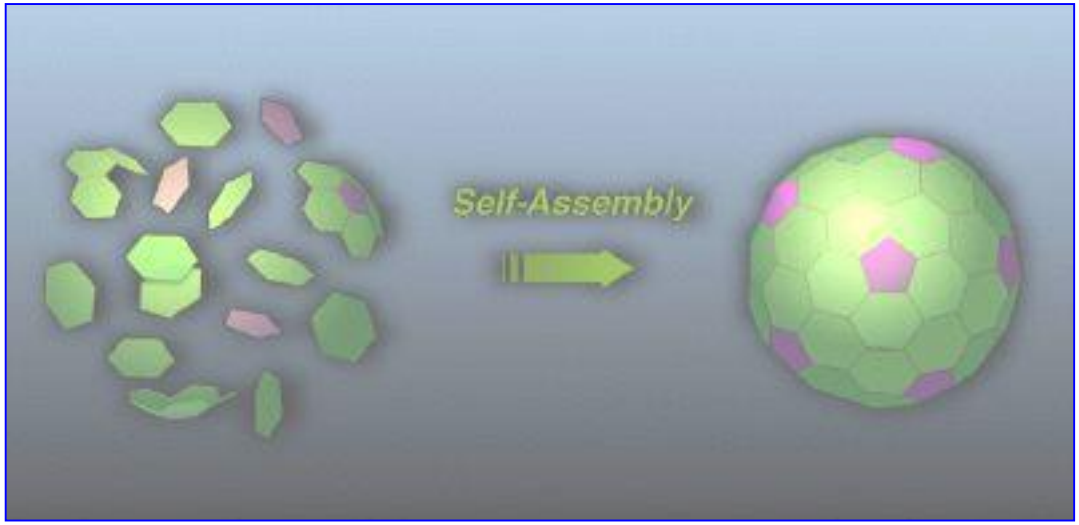

Metal-Ligand Interaction

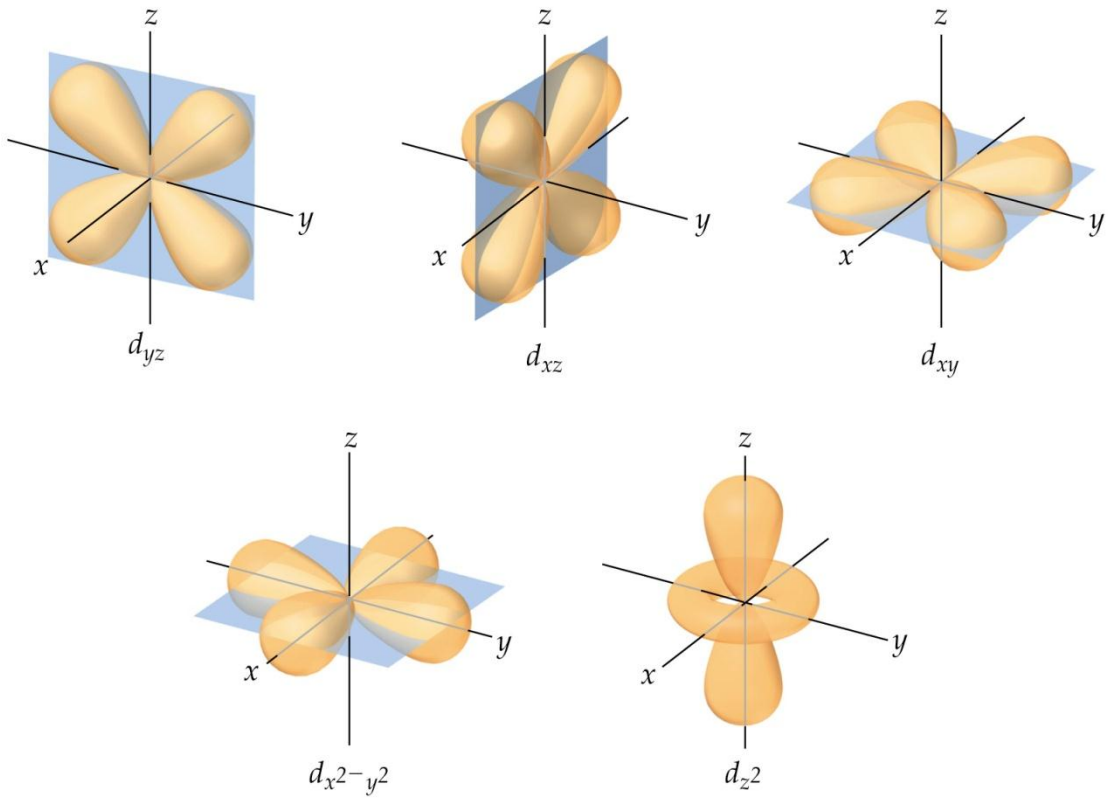

Metal as **connector** :

- labile M-L interaction (kinetic)
- stable compound (thermodynamic)
- highly directional with many geometries available

Metal as **functional group** :

- redox active (electron transfer)
- UV-vis active (color)
- photo active (phosphorescence)
- magnetic properties

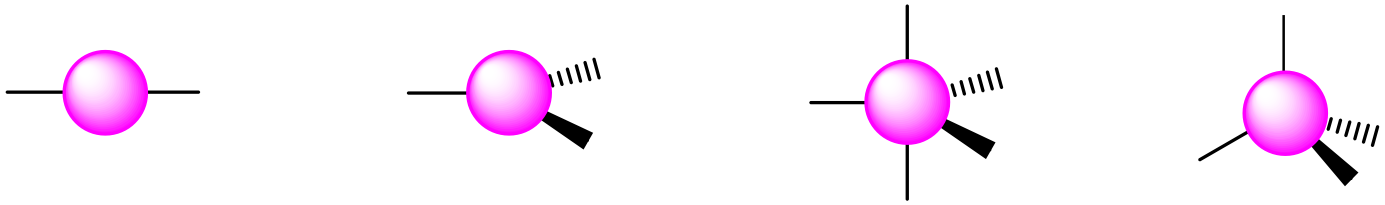

cis

Classical metals used:

Pd(II), Pt(II), Cu(I), Cu(II), Re(I), Co(II), Fe(II), Ag(I), Zn(II), Ru(II)…

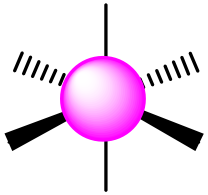

cis

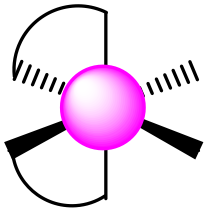

trans

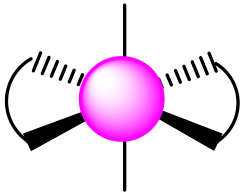

mer-

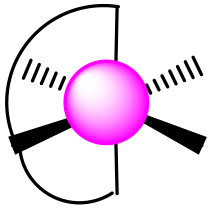

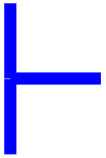

fac-

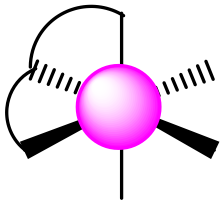

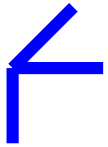

Supramolecular Coordination Chemistry

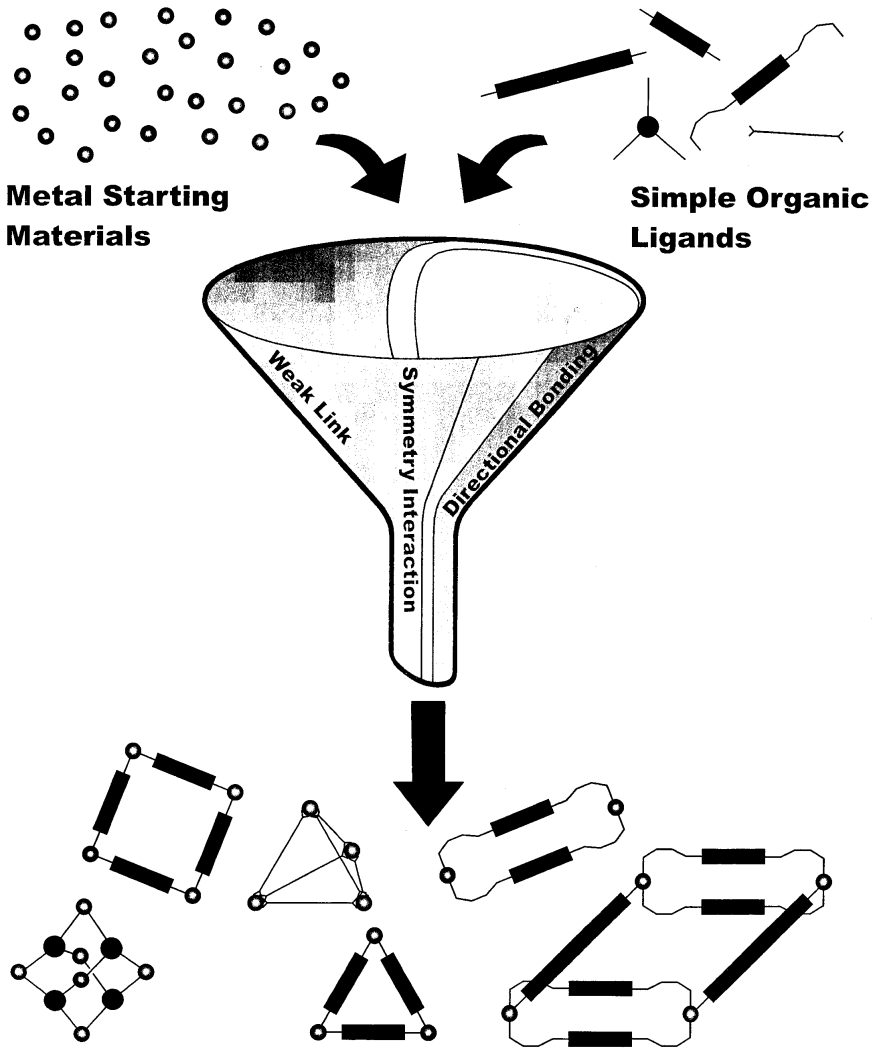

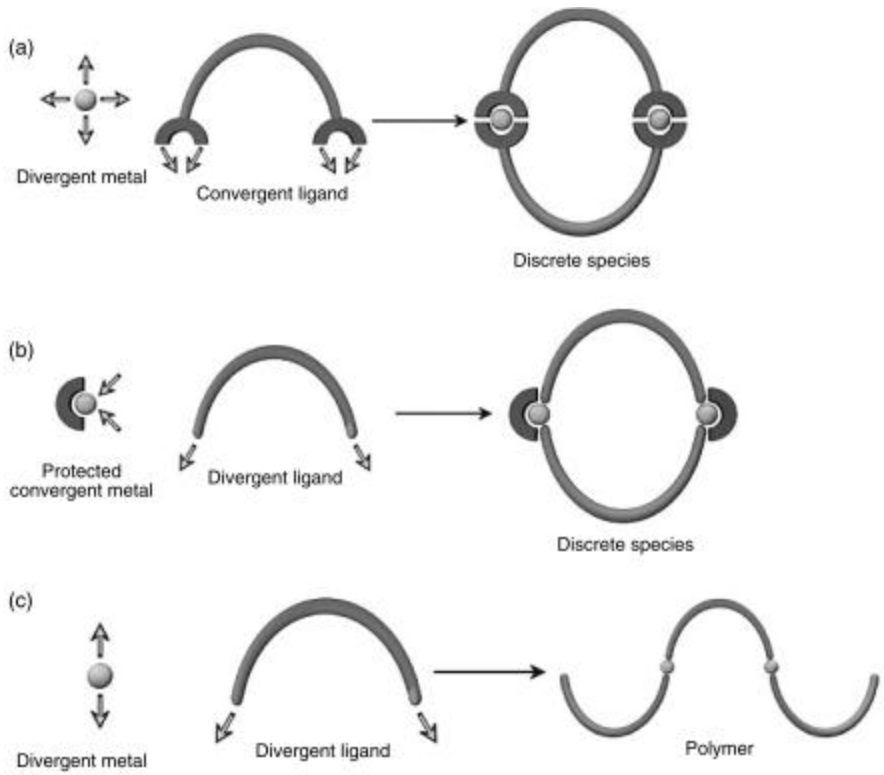
(a)
Divergent metal
Convergent ligand
Discrete species
(b)
Protected
convergent metal
Divergent ligand
Discrete species
(c)
Divergent metal
Divergent ligand
Polymer

Directonal Bonding Approach

M = bb acido, **L** = bb basico, definiti secondo il numero e geometria relativa dei siti acidi e basici

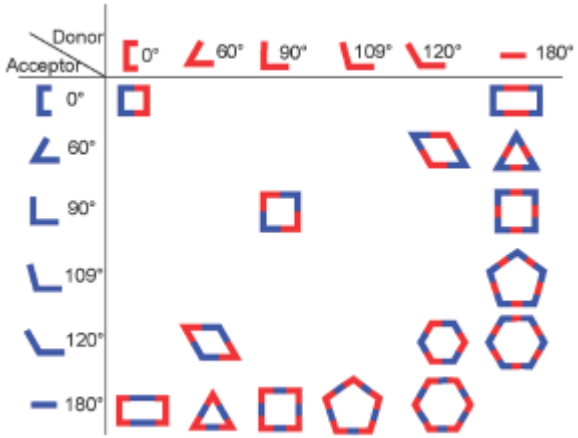

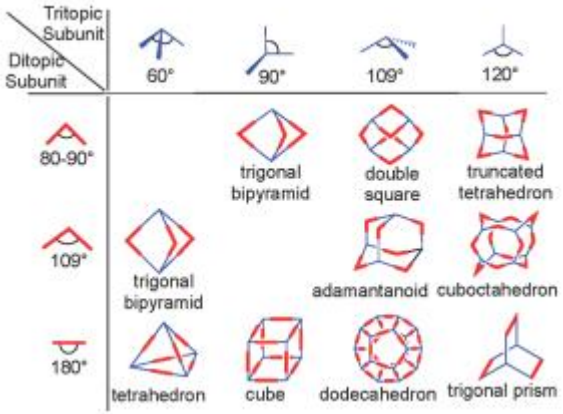

Specie poligonali 2D

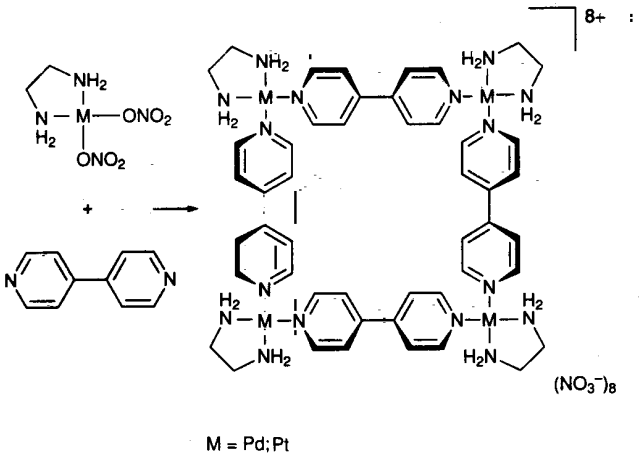

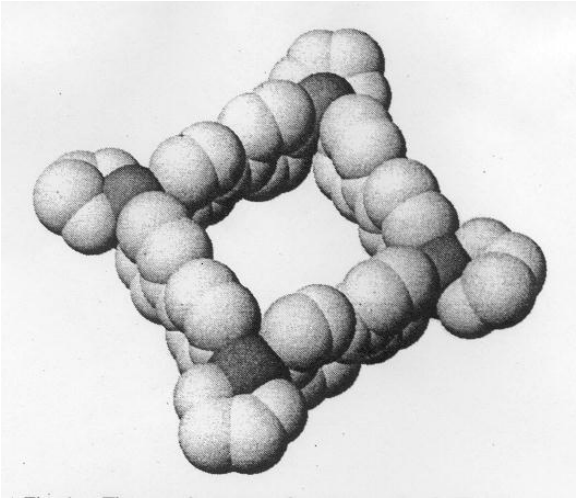

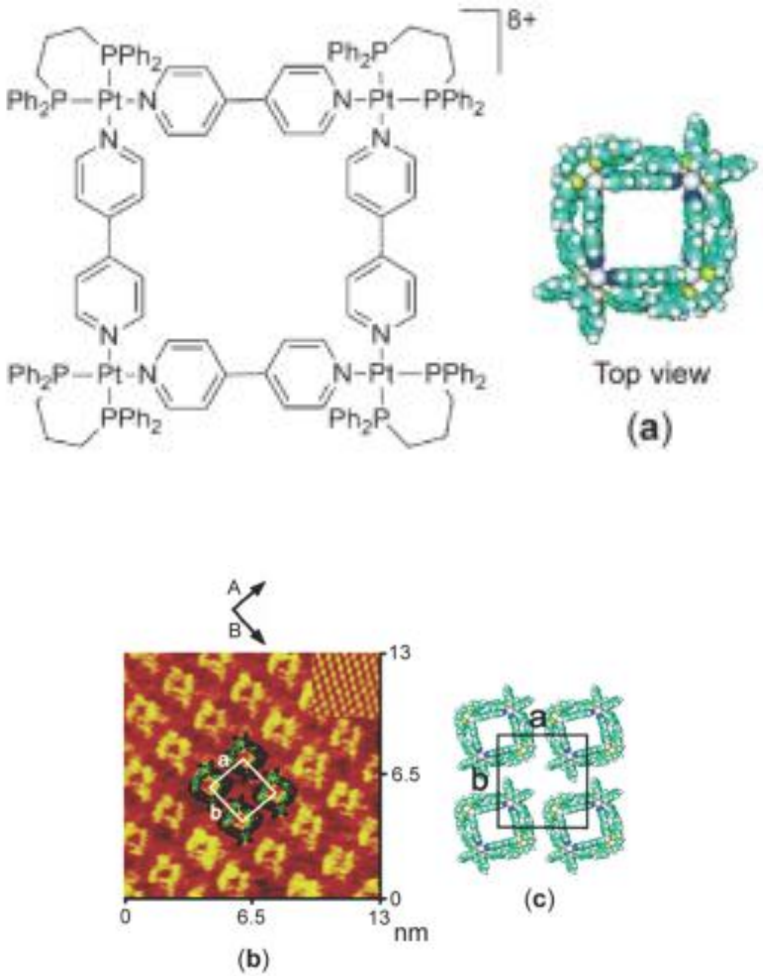

Figure 41. (a) Space-filling model of molecular square $[Pt(dppp)(4,4'\text{-bipyridine})]_4(PF_6)_8$, (b) high-resolution STM images of the adlayer of square on Au(111), and (c) structural model of the adlayer.

Triangoli Molecolari

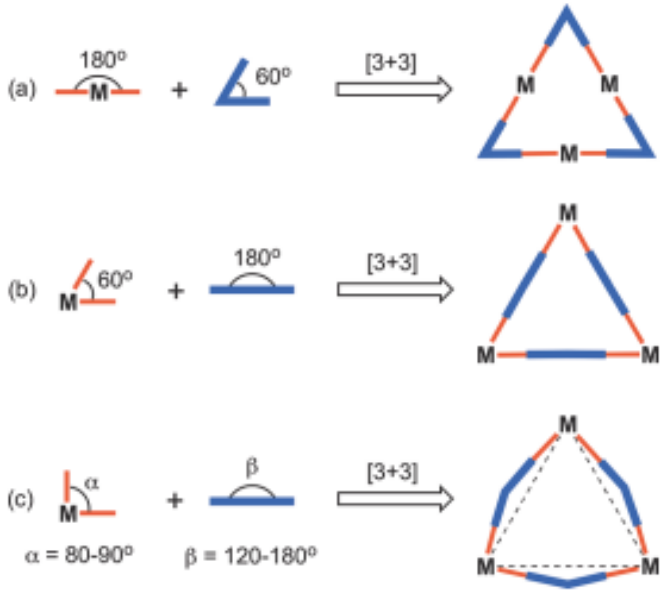

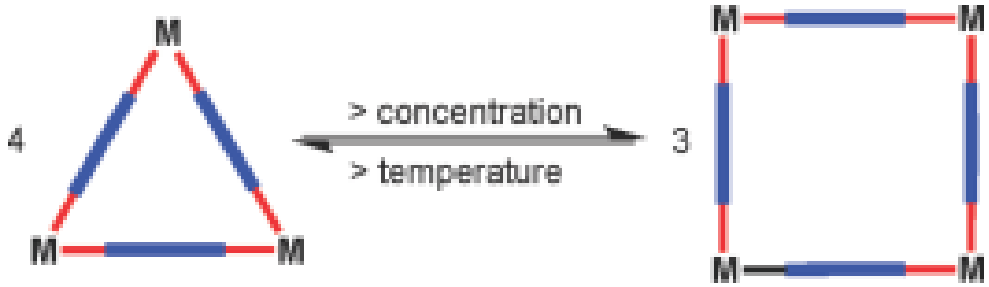

Square = Triangle endothermic $\Delta H < 0$
ΔS $< \Delta S$ < 0

Solvent
Concentration
Temperature

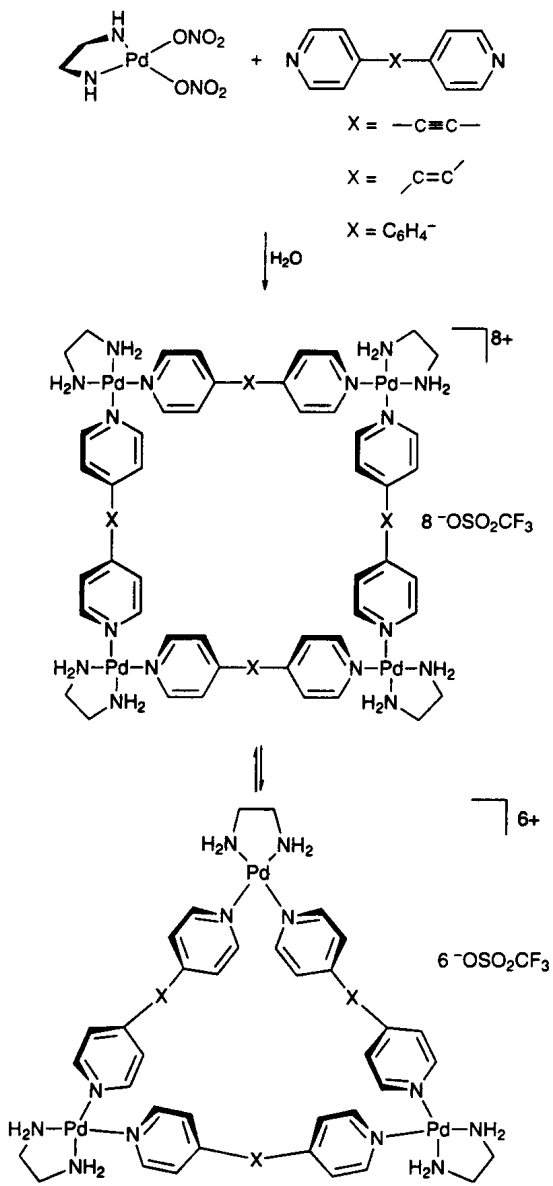
X = —C≡C—
X = C=C
X = C6H4
H2O
8+
8 ⁻OSO2CF3
6+
6 ⁻OSO2CF3

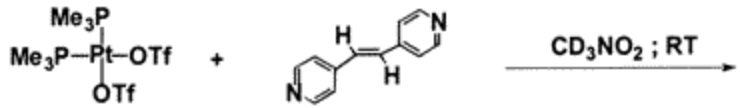

1 2

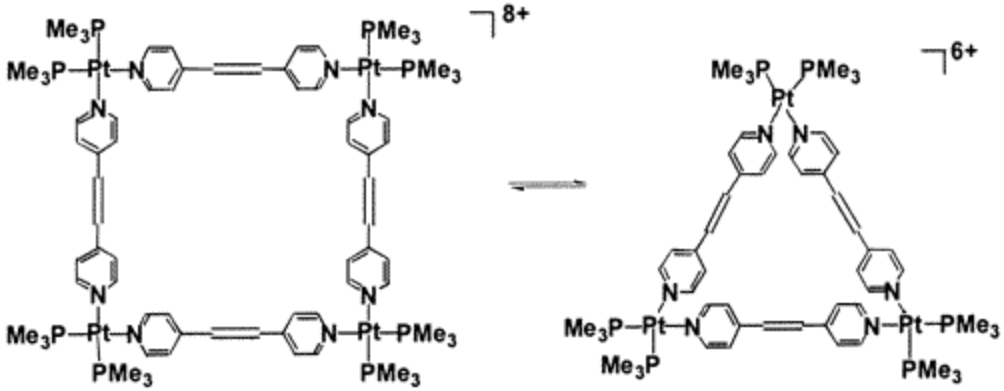

8 $CF_3SO_3^-$ 6 $CF_3SO_3^-$

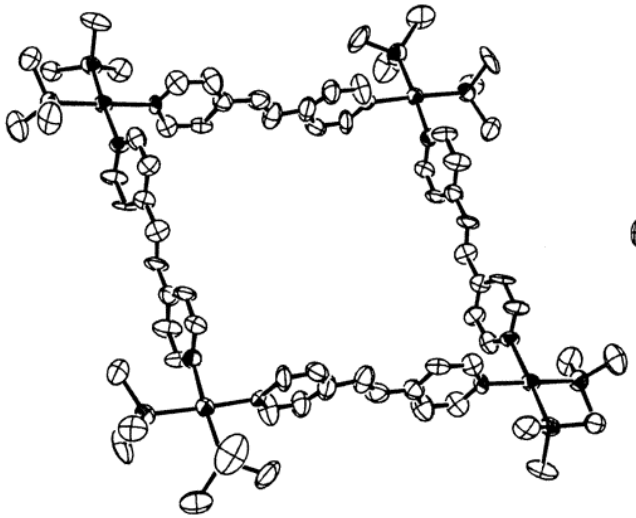

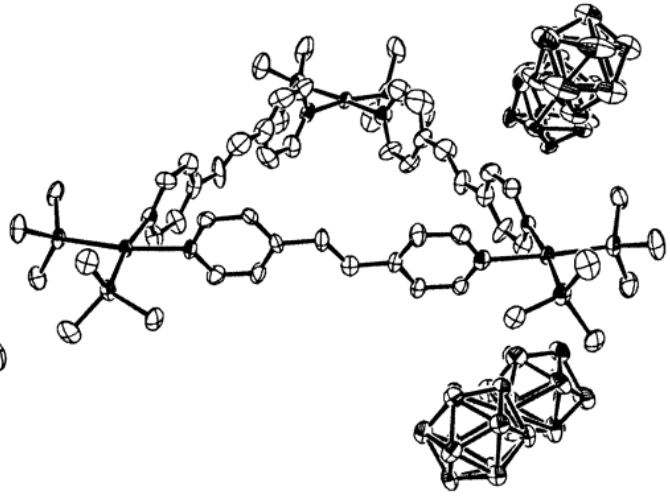

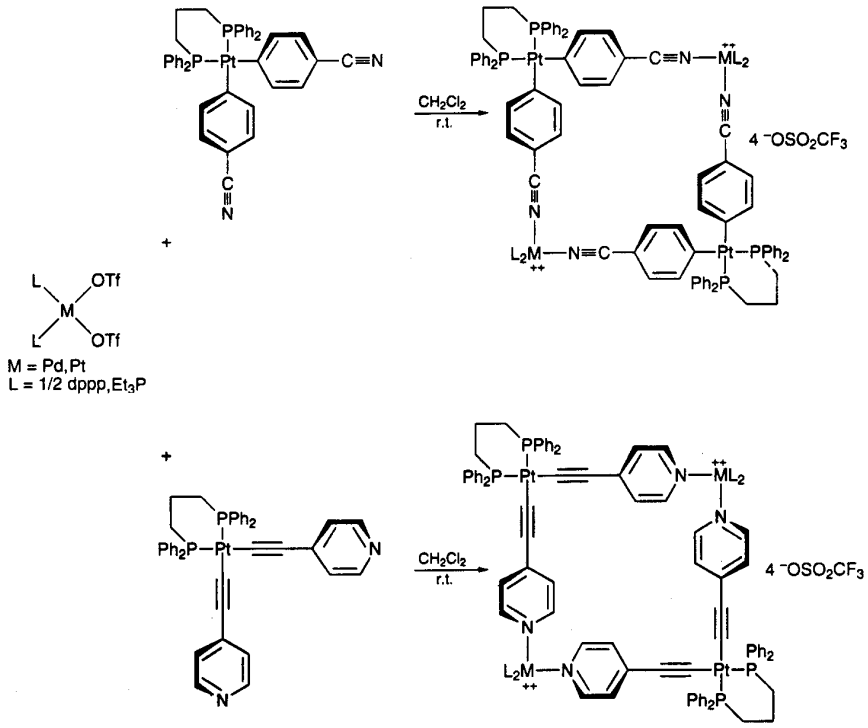
M = Pd,Pt
L = 1/2 dppp,Et3P
CH2Cl2
r.t.
4 ⁻OSO2CF3

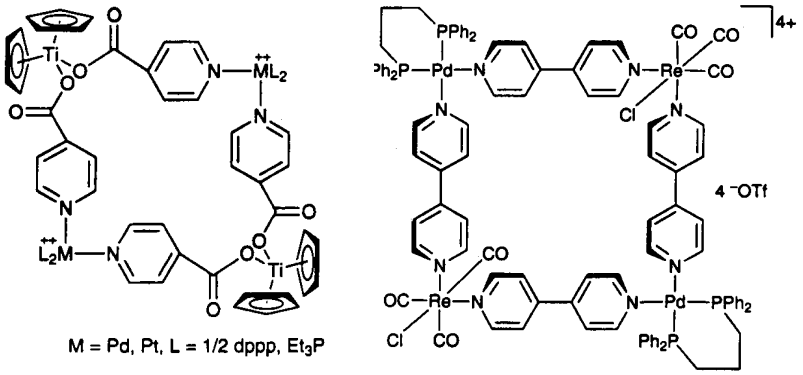
M = Pd, Pt, L = 1/2 dppp, Et3P
4 ⁻OTf
4+

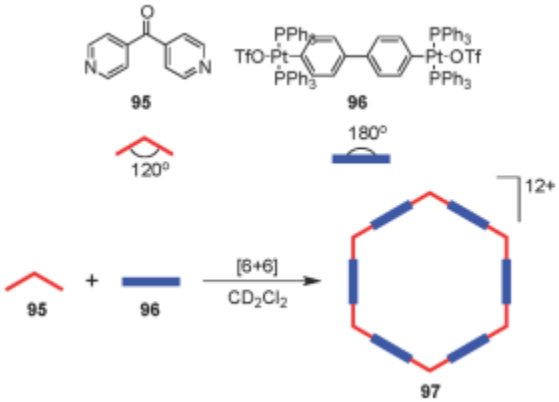
95
96
120°
180°
12+
[6+6]
CD_2Cl_2
97

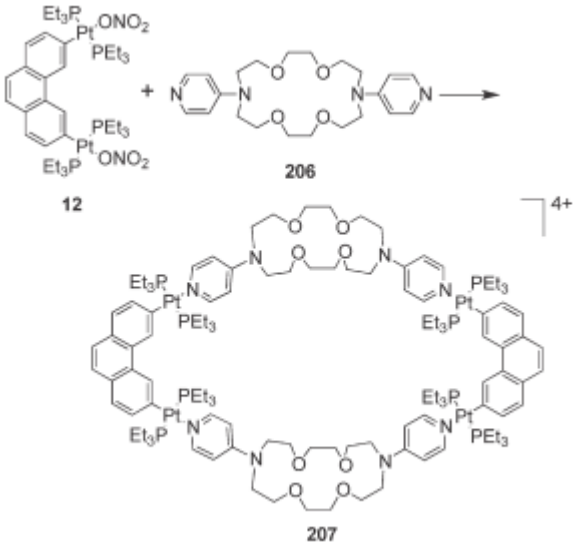
12
206
4+
207

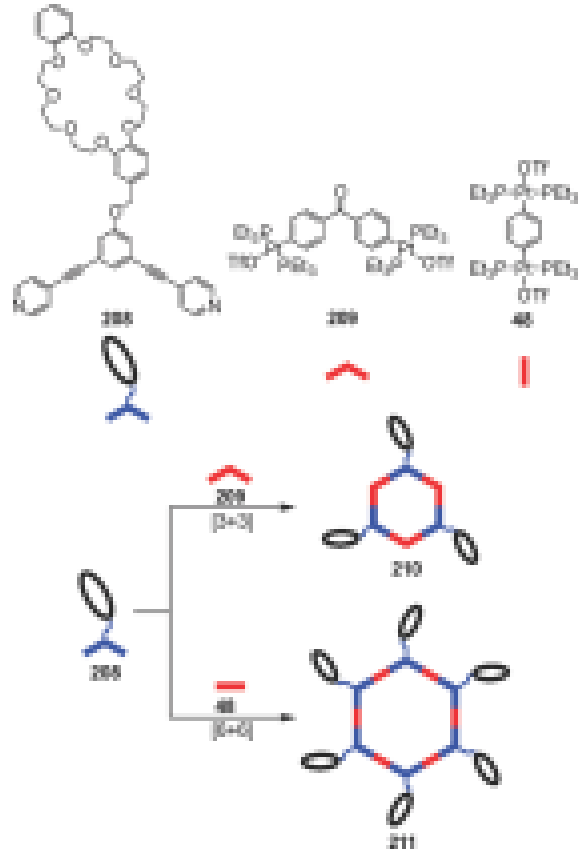
[3+3]
[6+6]
210
211

Directonal Bonding Approach

M = bb acido, **L** = bb basico, definiti secondo il numero e geometria relativa dei siti acidi e basici

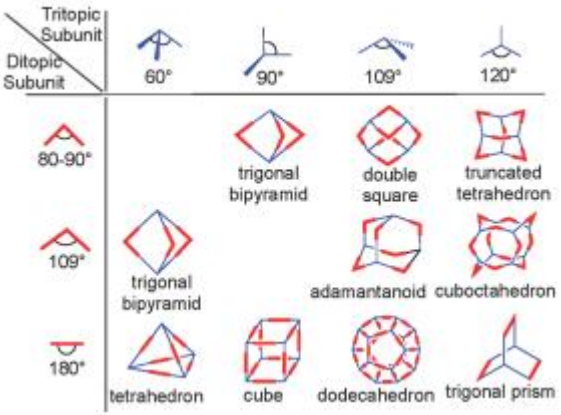

Gabbie Molecolari

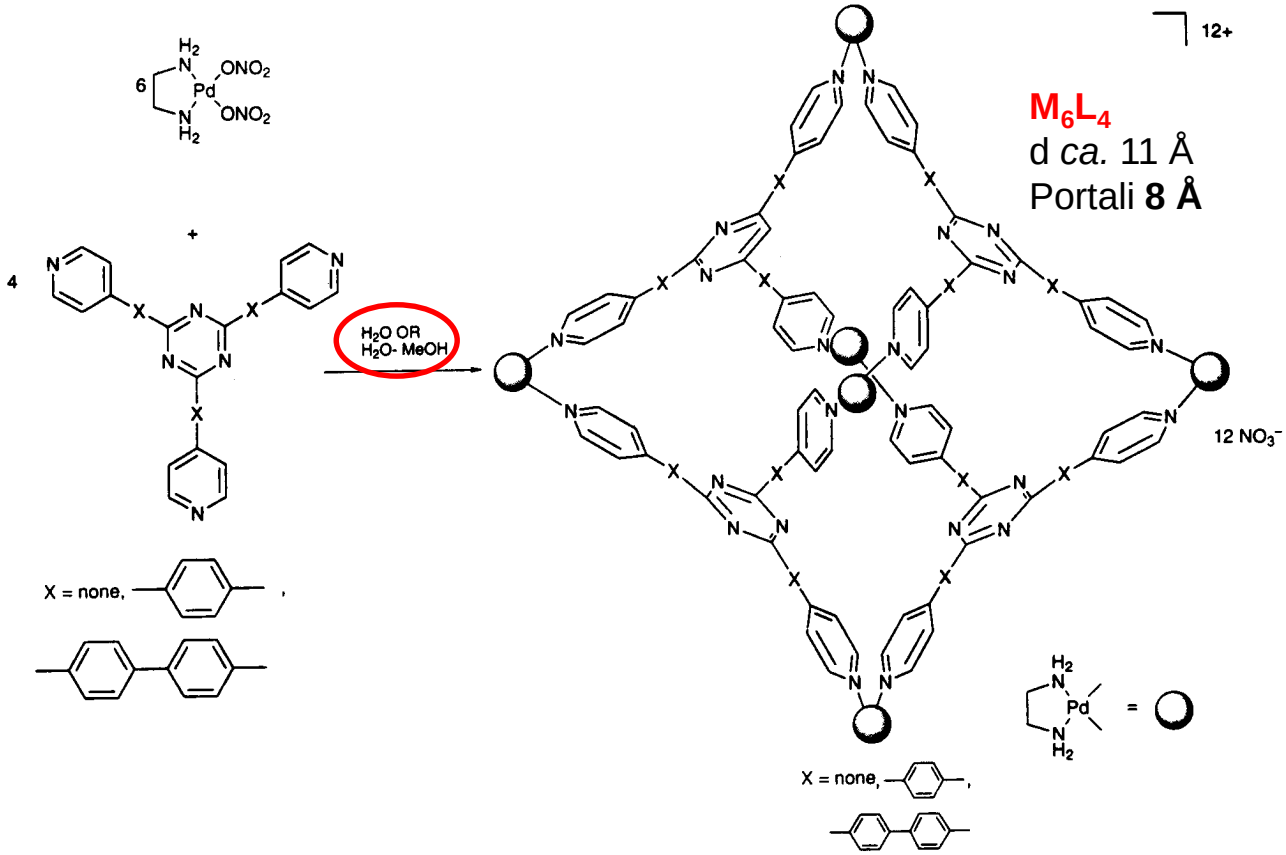

M_6L_4
d *ca.* 11 Å
Portali **8 Å**

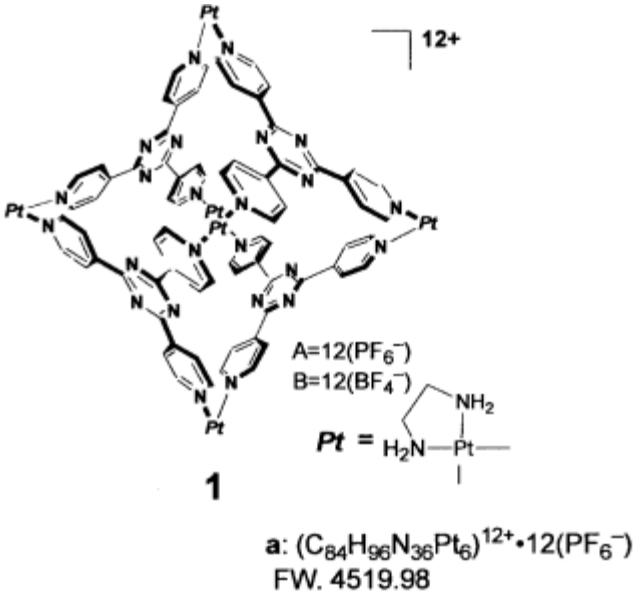

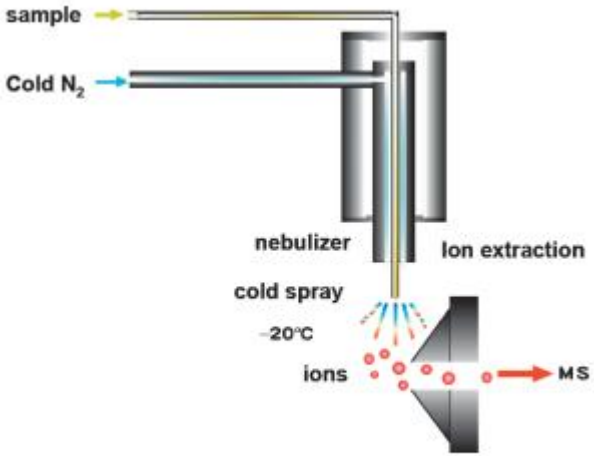

Fig. 1. Schematic illustration of the cold spray.

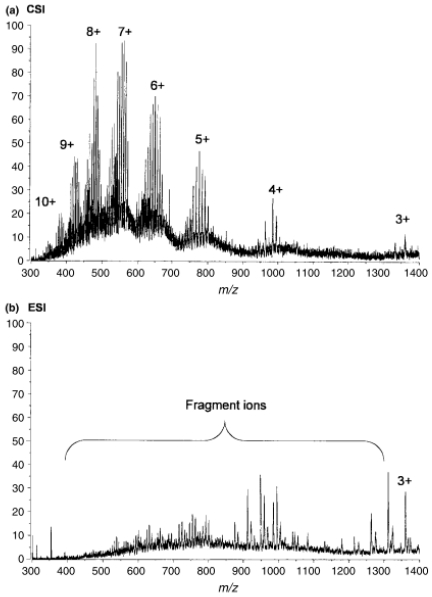

Figure 3. Comparison of (a) CSI and (b) ESI mass spectra of **1a**. Reprinted from Ref. 2 with permission from Elsevier.

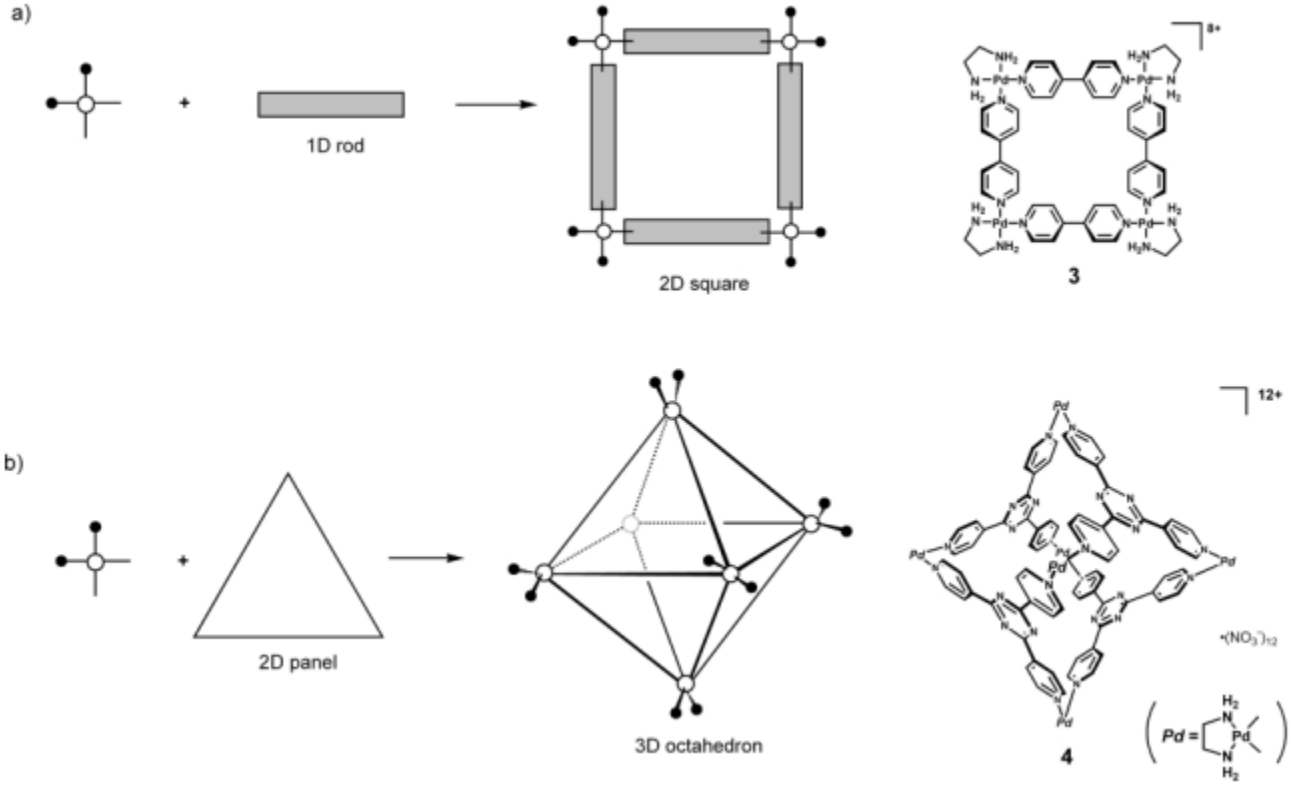
a)
1D rod
2D square
3
b)
2D panel
3D octahedron
4
12+
•(NO3⁻)12
Pd =

Molecular Paneling

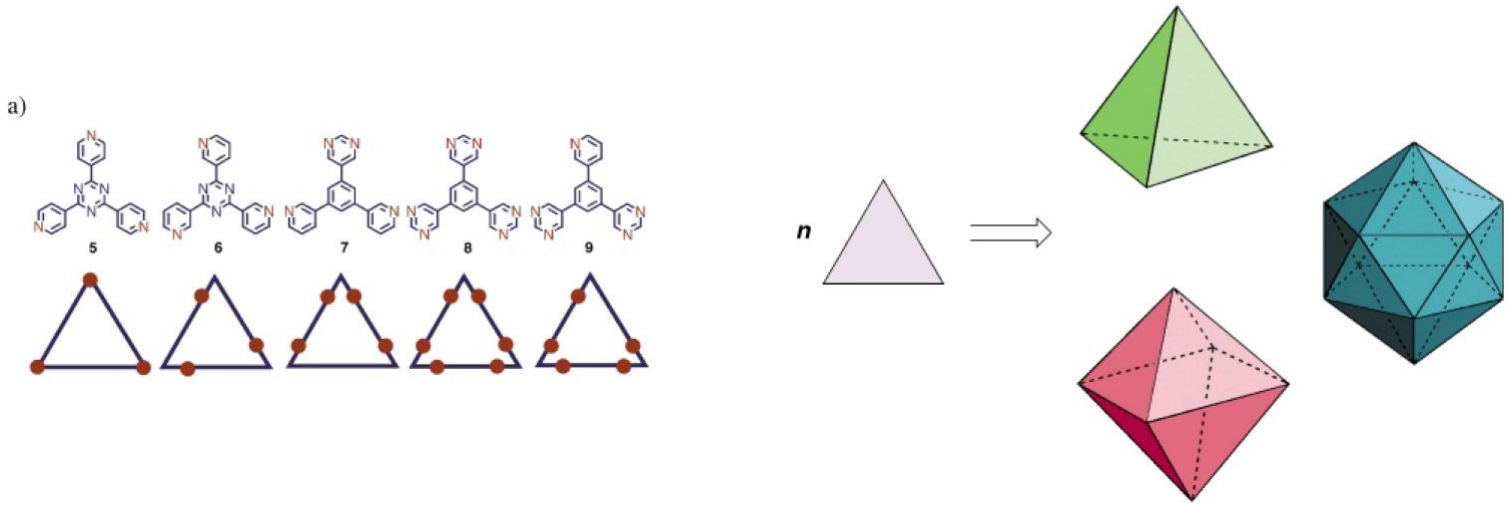

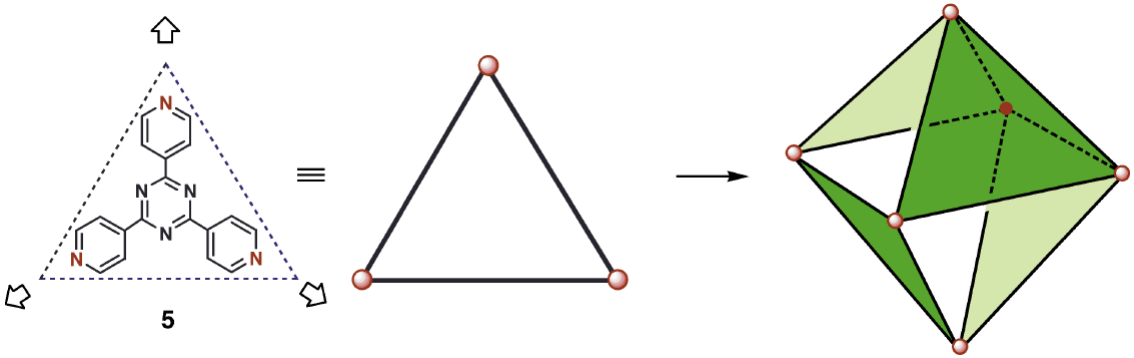

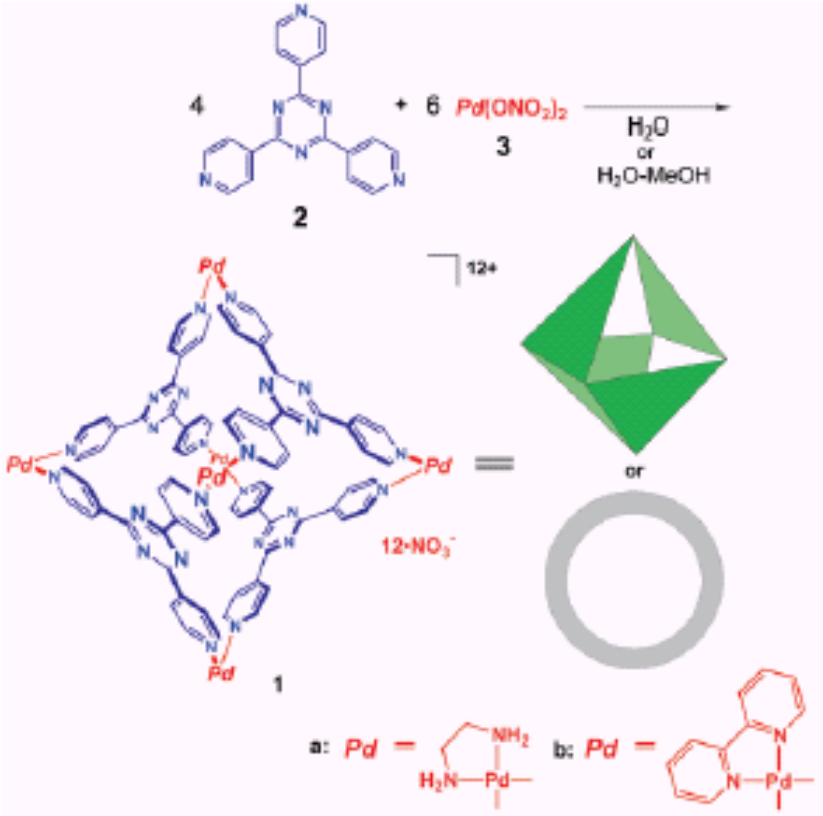
4
+ 6 Pd(ONO2)2
3
H2O
or
H2O-MeOH
2
12+
Pd
12·NO3-
or
1
a: Pd =
b: Pd =

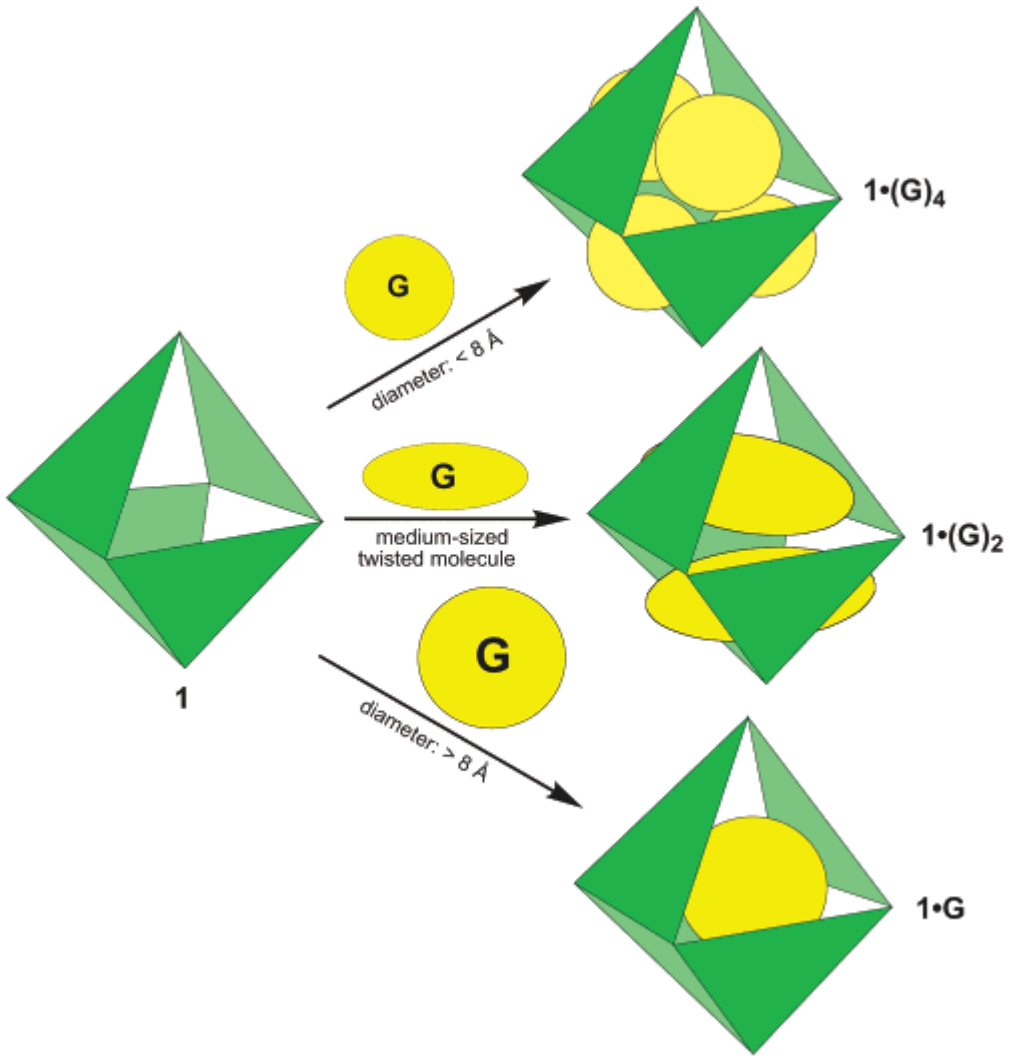
G
diameter: < 8 Å
1•(G)4
G
medium-sized
twisted molecule
1•(G)2
G
diameter: > 8 Å
1•G
1

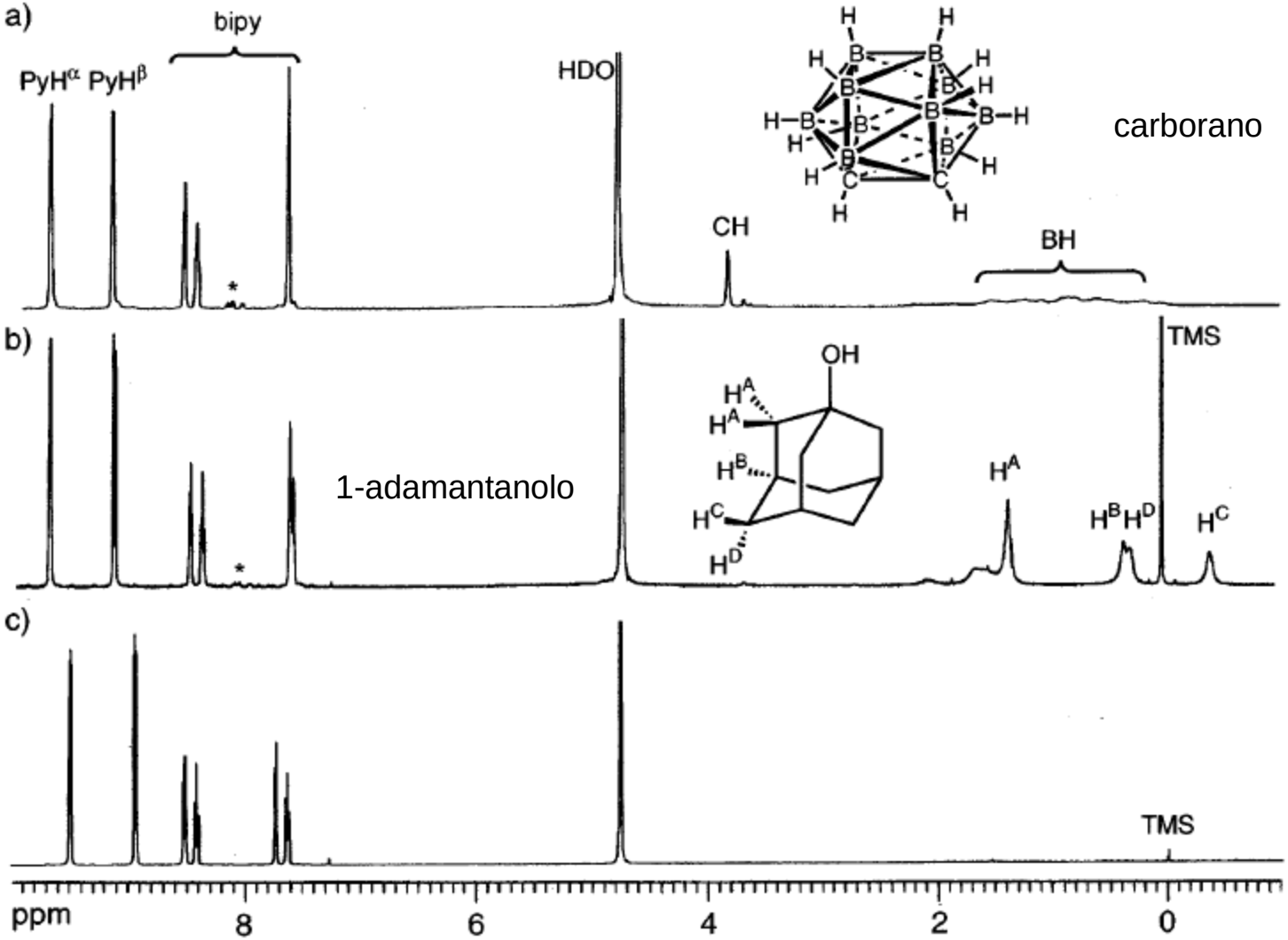

Figure 1. ^{1}H NMR observations of the enclathration of guest molecules in **1b**. (a) **1b**·(**4**)$_4$. (b) **1b**·(**5**)$_4$. (c) Empty **1b** (*: impurities).

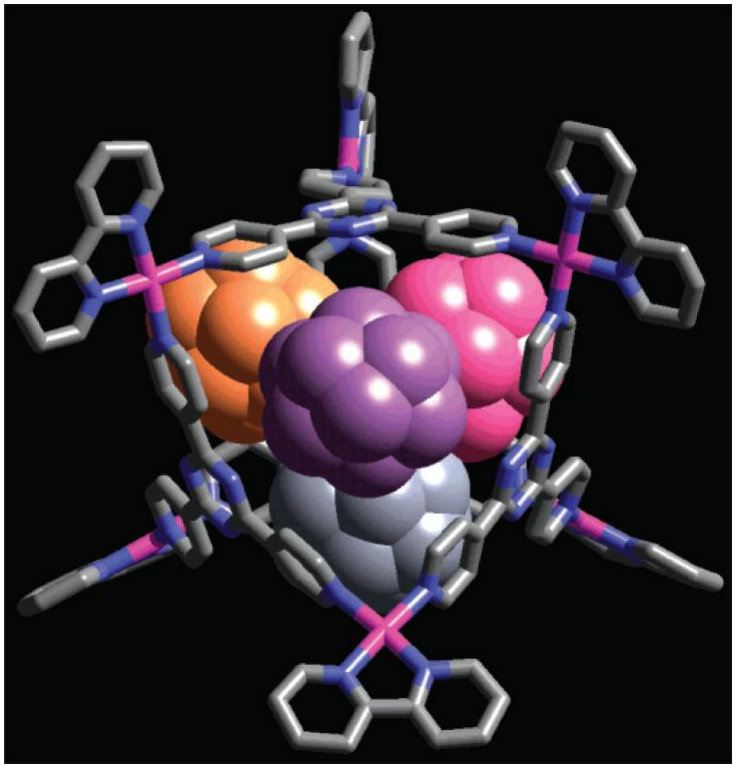

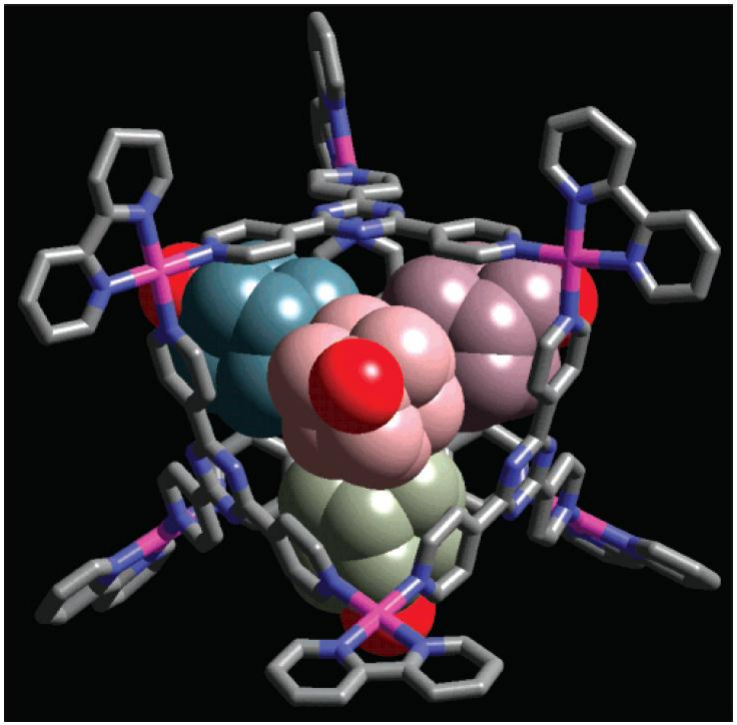

Scheme 2

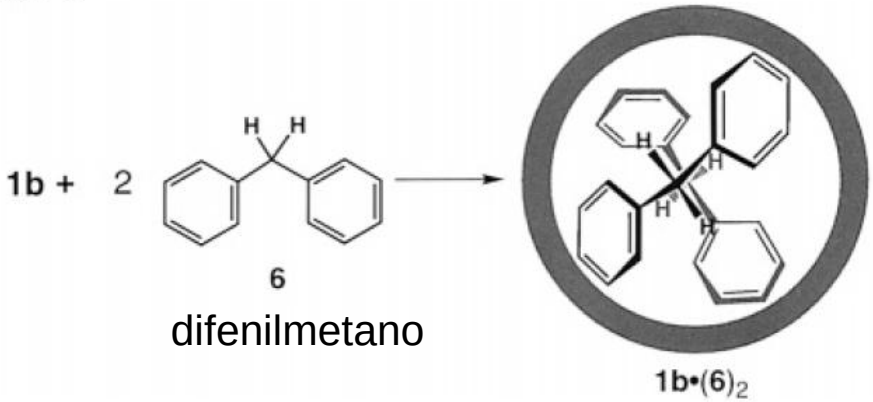

difenilmetano

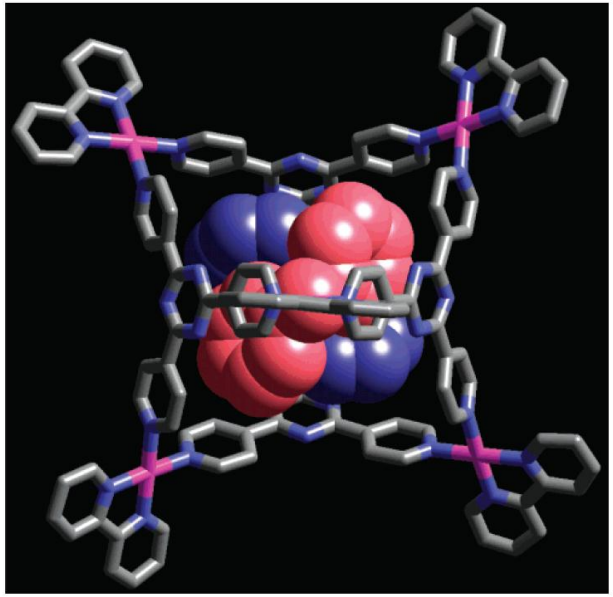

cis-azobenzene

cis-stilbene

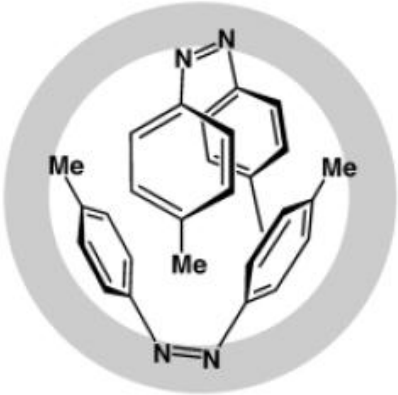

Scheme 3

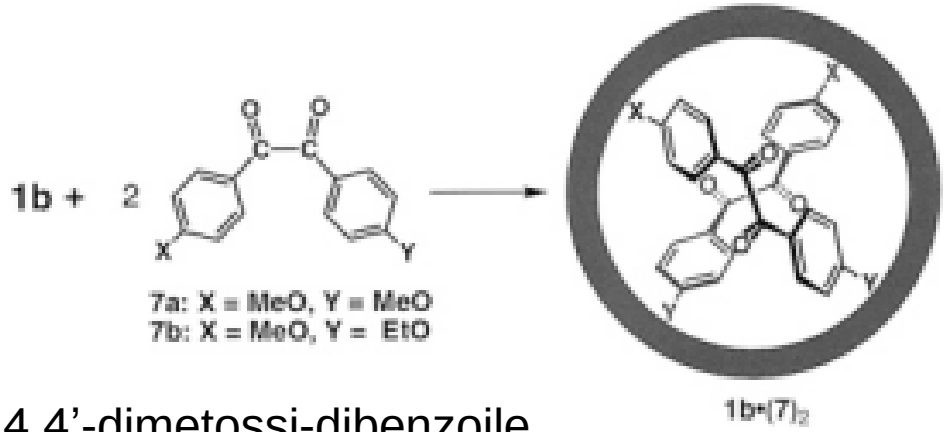

4,4’-dimetossi-dibenzoile

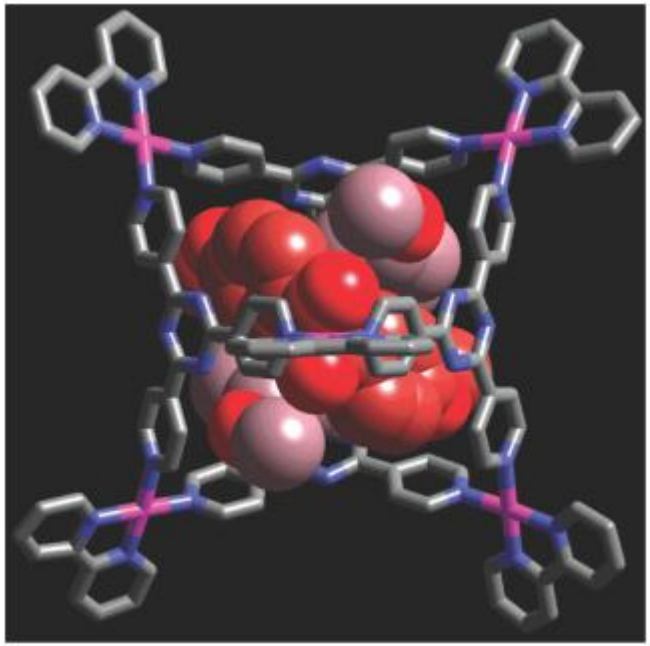

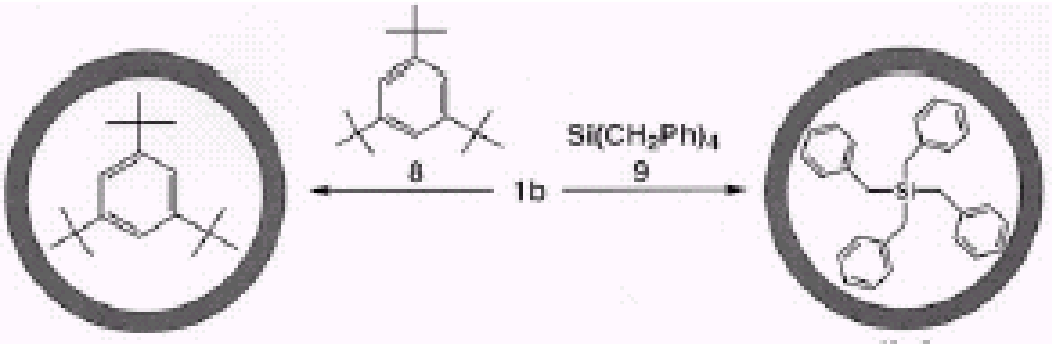

tri-*tert*-butilbenzene **tetrabenzilsilano**

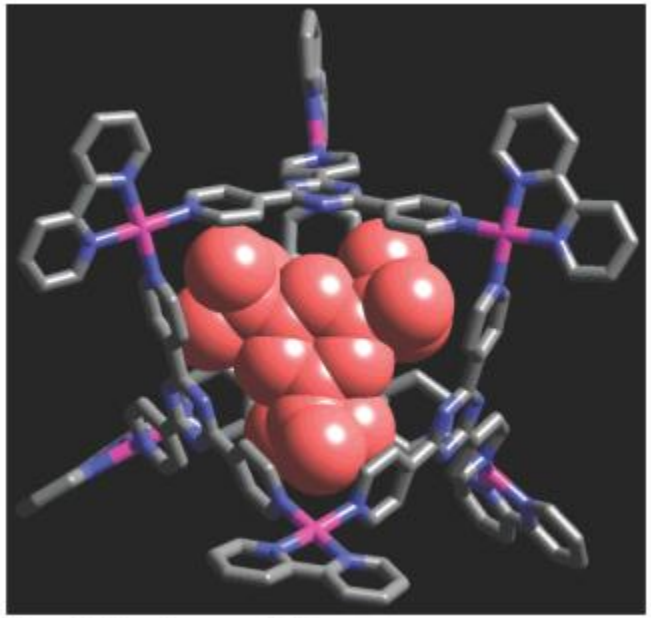

Figure 8. Crystal structure of **1b·8**.

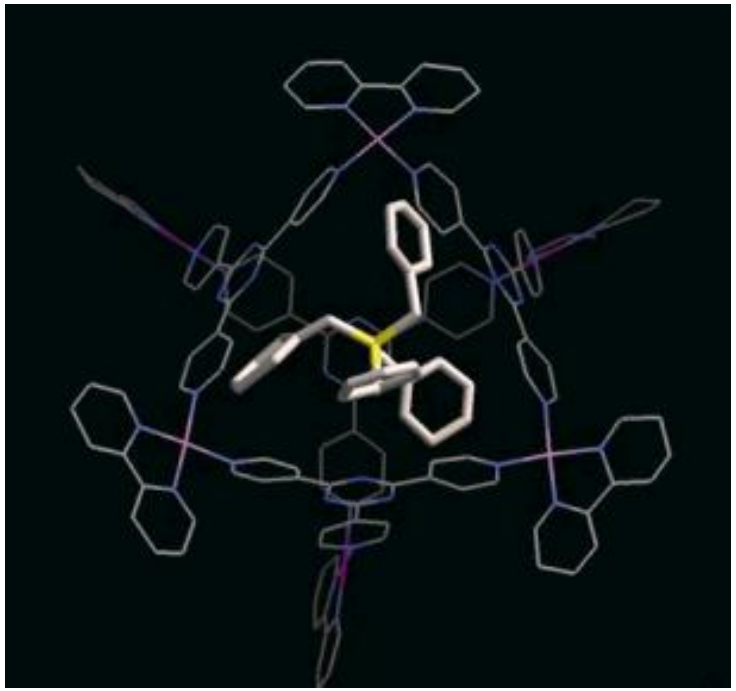

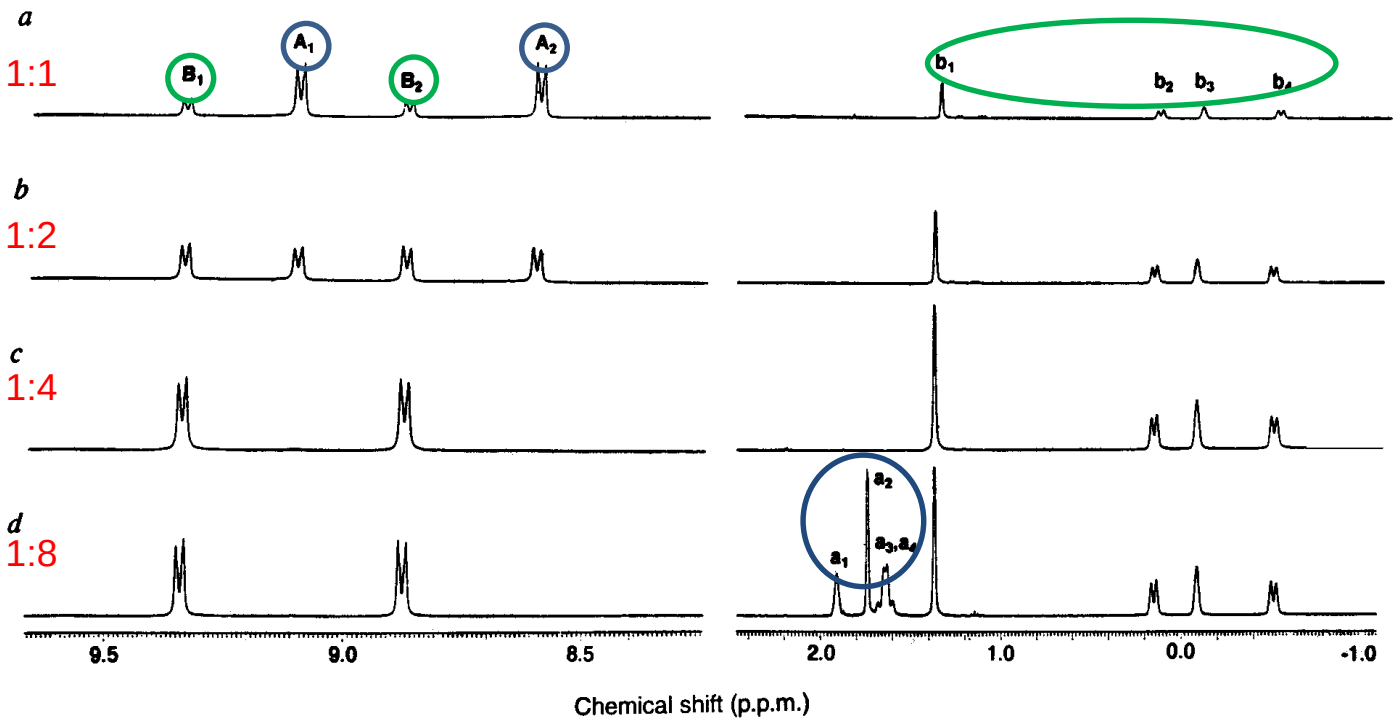

M_6L_4/adamantancarbossilato$_4$

Effetto allosterico!

a)

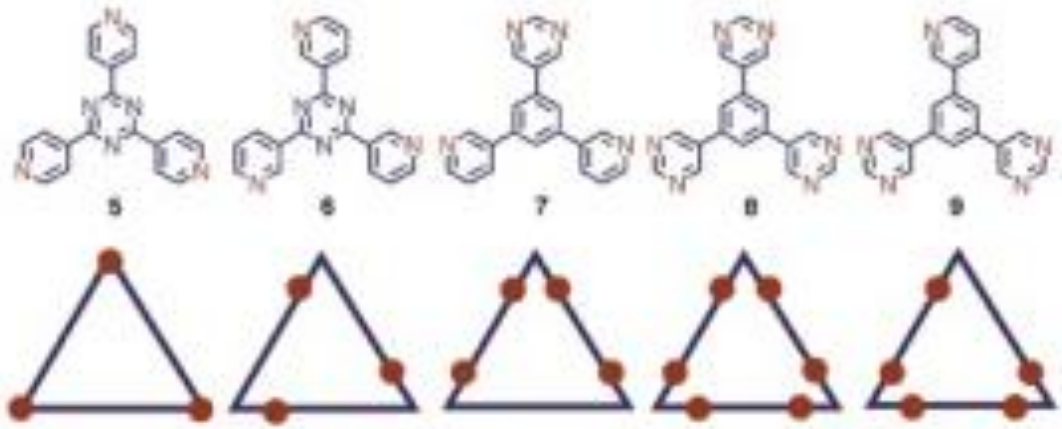

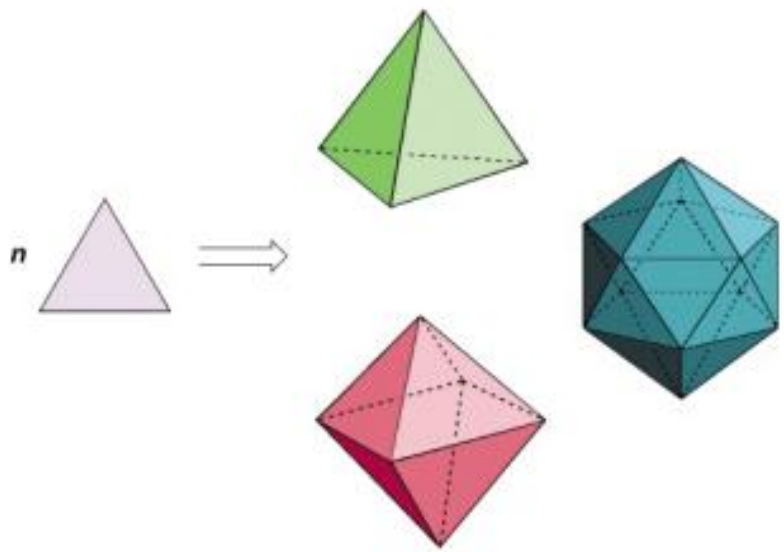

a)

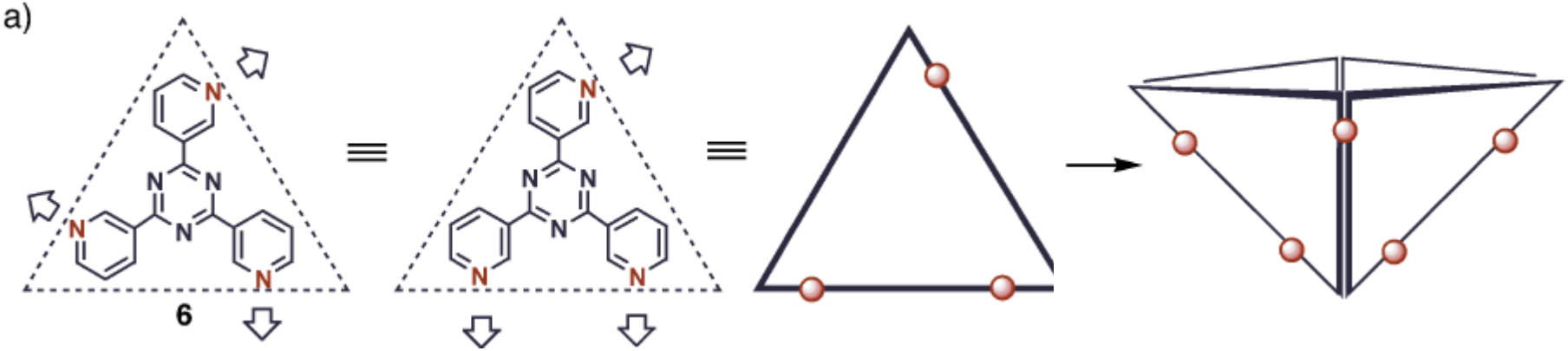

b)

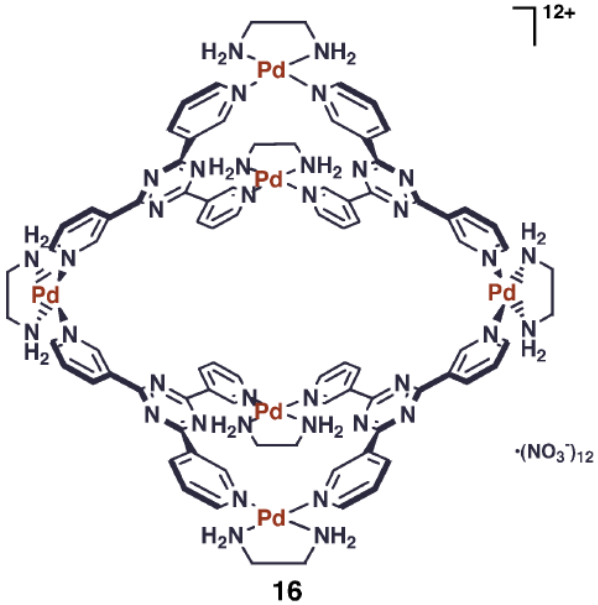

c)

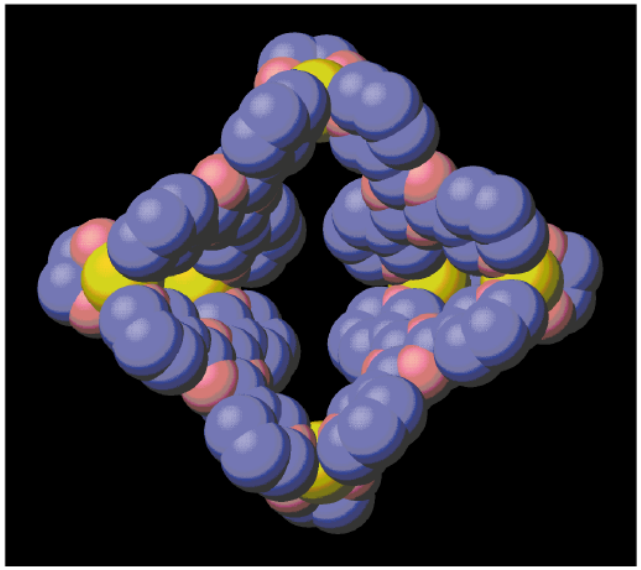

a)

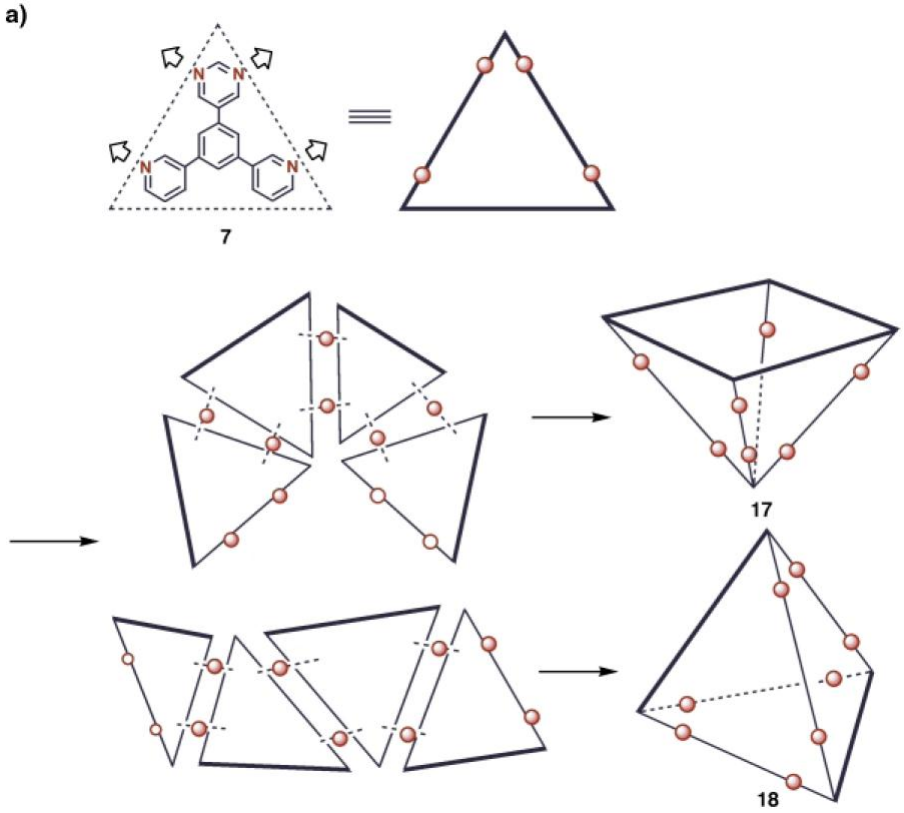

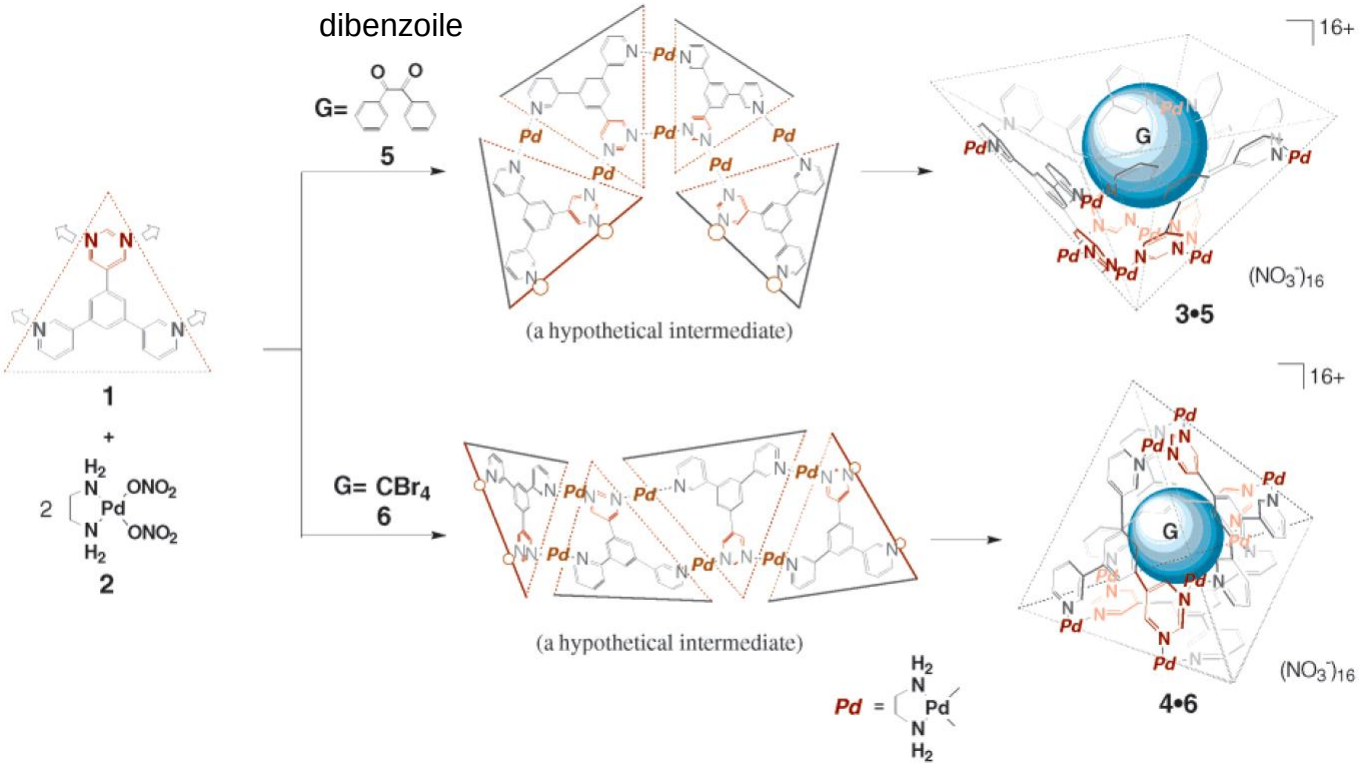
dibenzoile
G=
5
1
+
2
G= CBr4
6
(a hypothetical intermediate)
(a hypothetical intermediate)
16+
3•5
4•6
(NO3-)16
Pd =

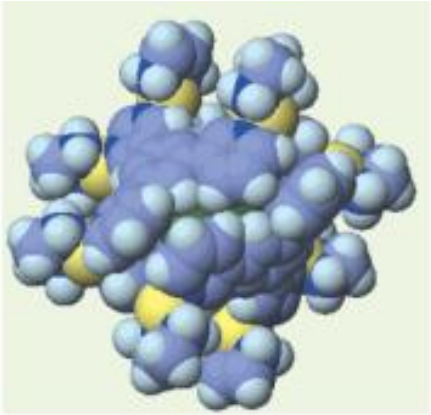

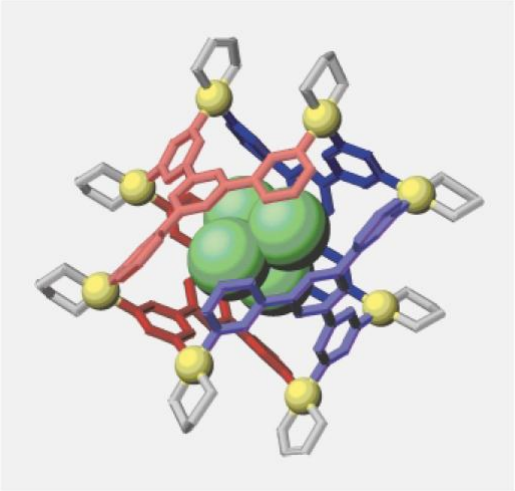

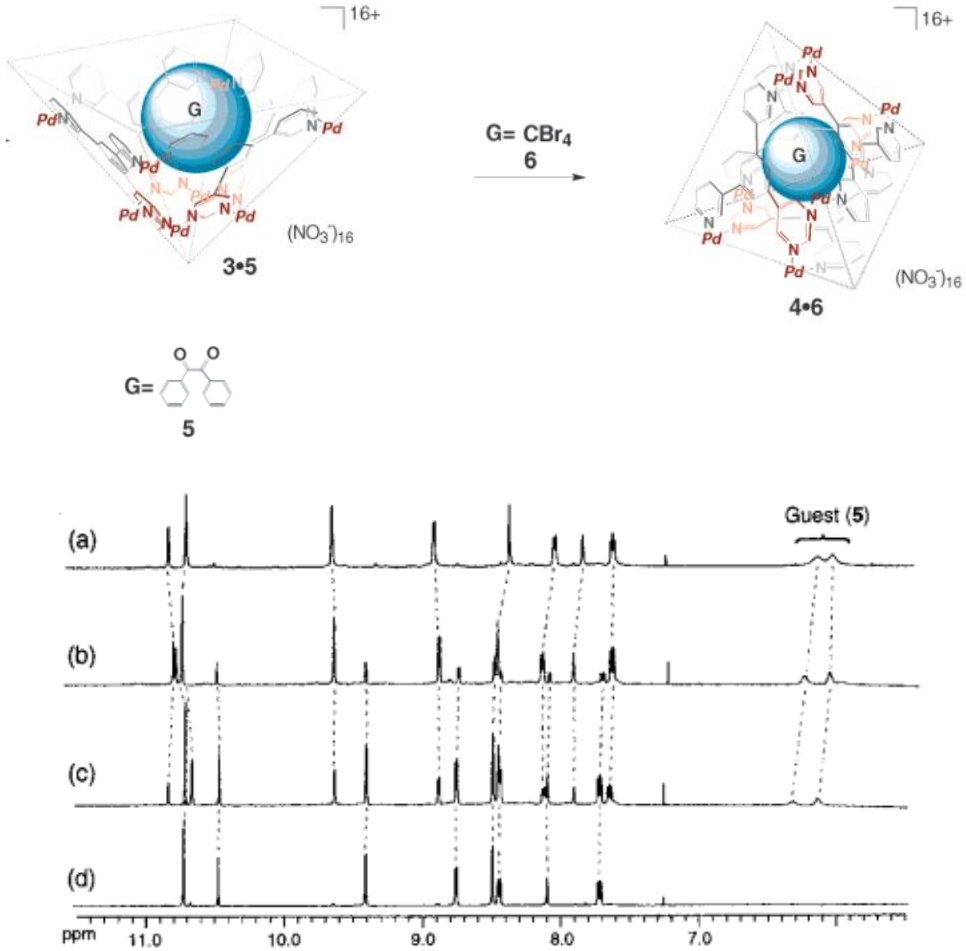

Figure 2. The ^{1}H NMR monitoring of reorganization process from **3·5** to **4·6** via guest exchange. (a) **3·5** complex in D_2O; (b−d) After the addition of excess amount of **6** at 25 °C ((b) 3 h, (c) 8 h, (d) 24 h). Note that free **5** is immiscible in water and, after guest exchange, becomes invisible in the spectrum.

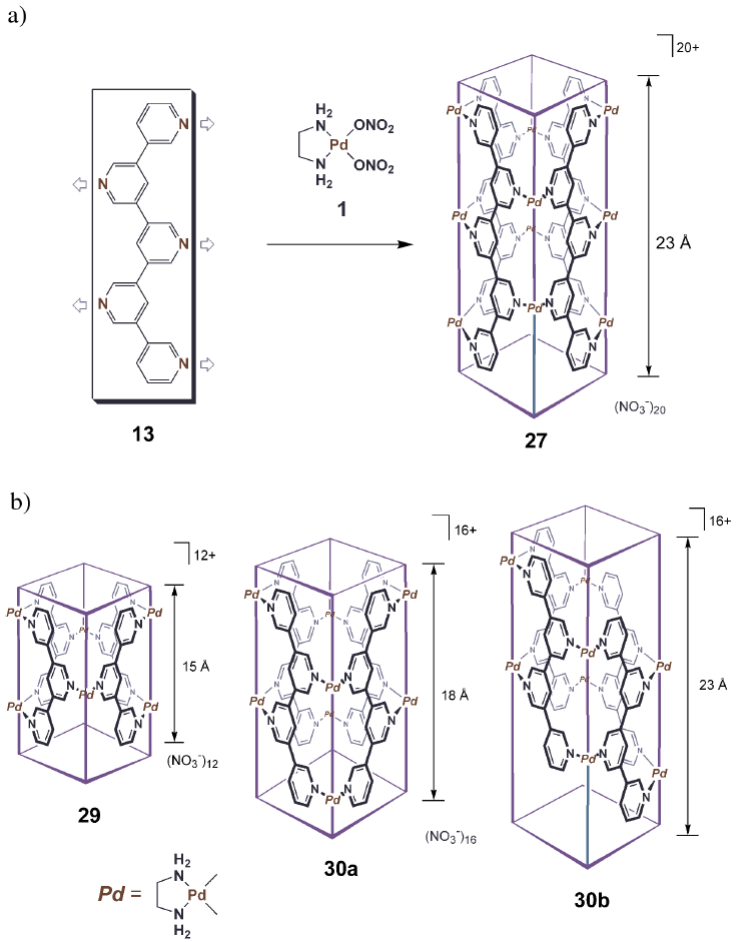
a)
13
1
27
20+
23 Å
$(NO_3^-)_{20}$
b)
29
12+
15 Å
$(NO_3^-)_{12}$
30a
16+
18 Å
$(NO_3^-)_{16}$
30b
16+
23 Å
Pd =

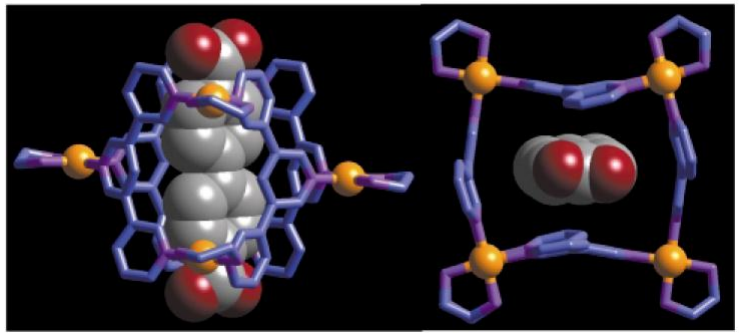

Stabilizzazione di intermedi reattivi: alcossi-silani ciclici
Ship in a Bottle

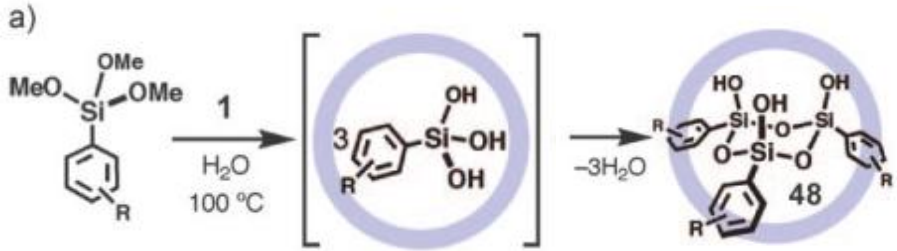

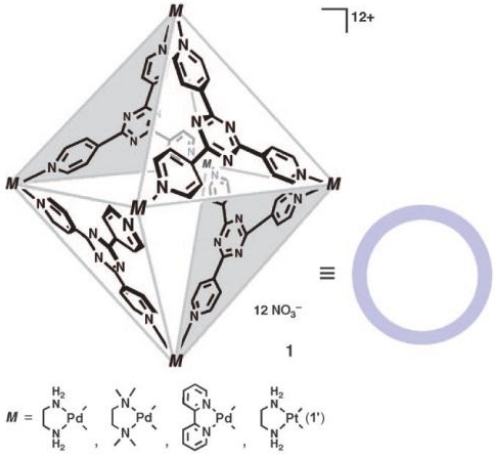

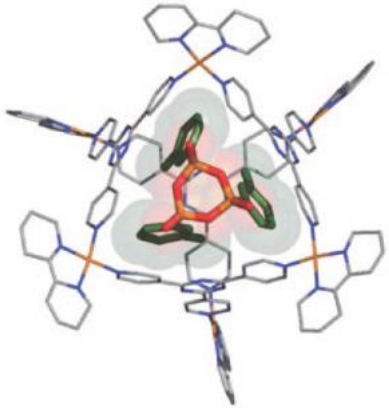

Stabilizzazione di intermedi reattivi: Oligomerizzazione di tri alcossi-silani

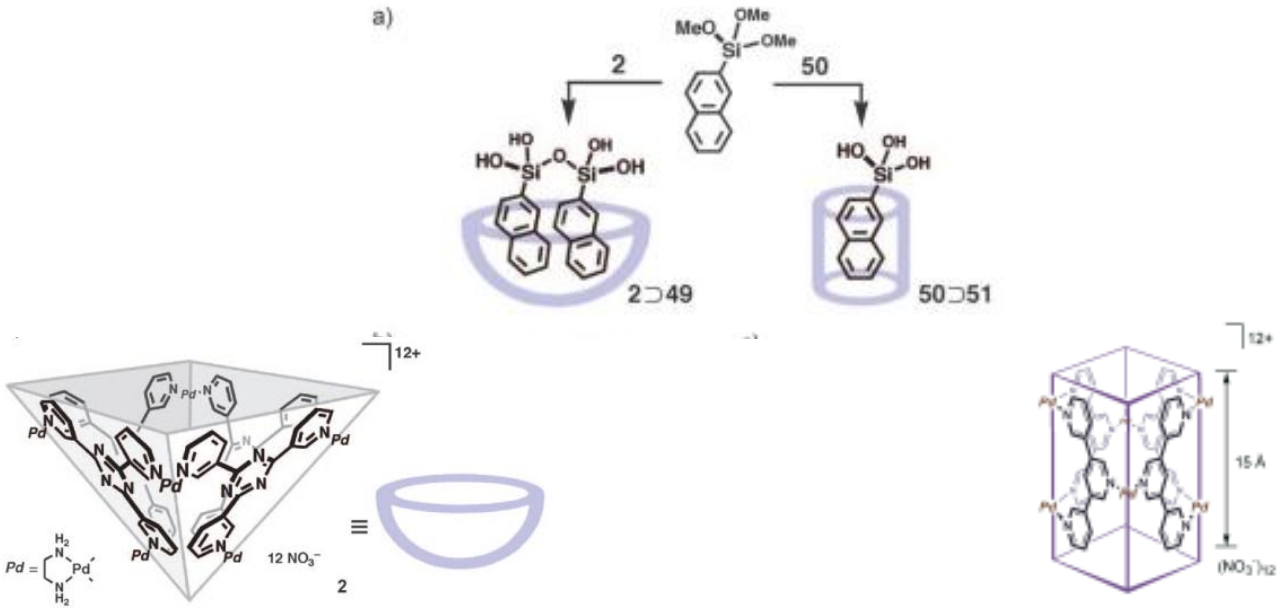

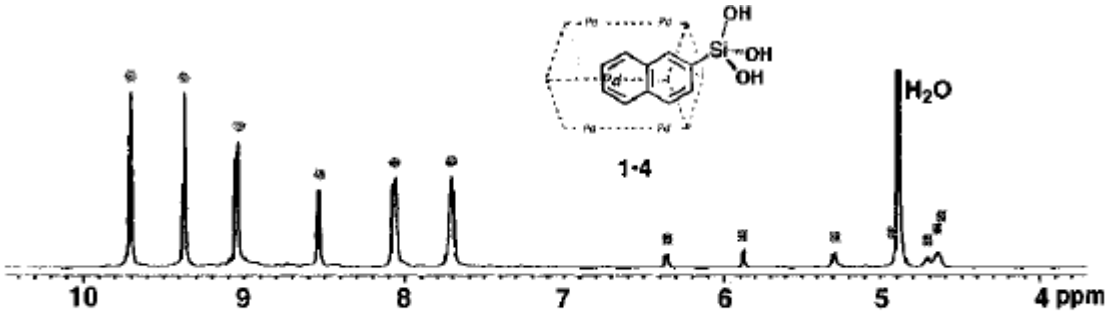

Figure 1. ^{1}H NMR spectrum (500 MHz, D_2O, TMS as an external standard) of **1·4** at 27 °C. Circles and squares indicate host and guest signals, respectively.

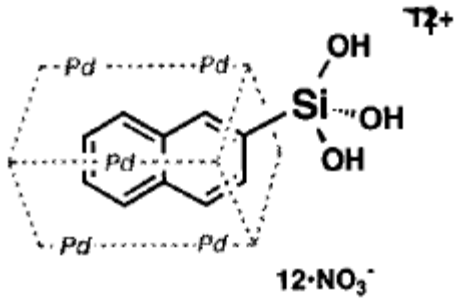

1·4

^{29}Si NMR of 1·4

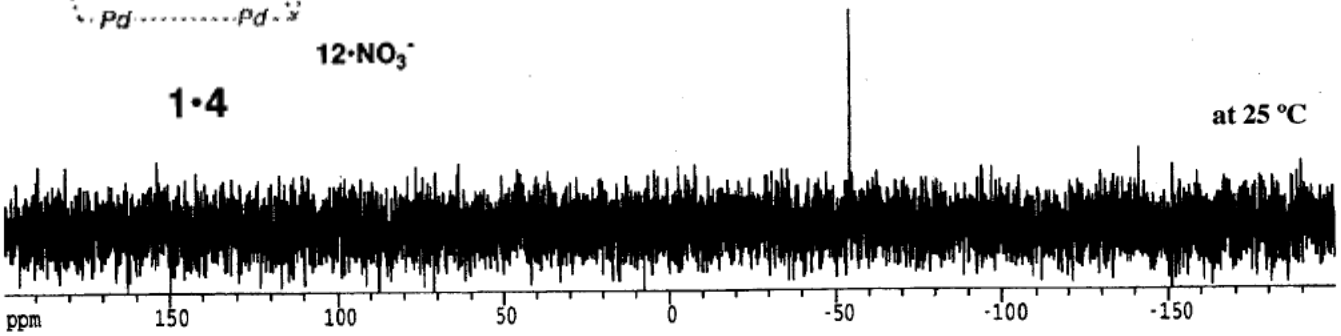

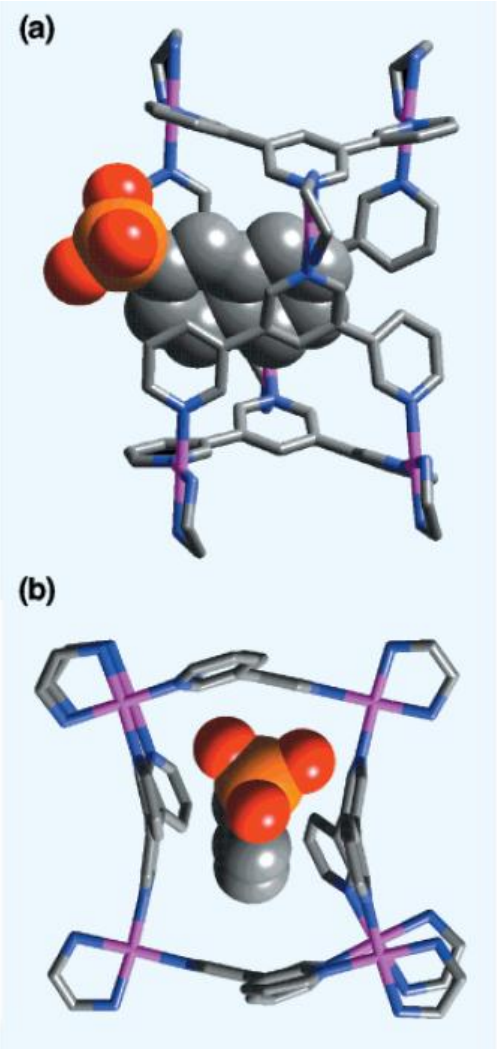

Figure 2. The crystal structure of **1·4**: (a) side view and (b) top view.

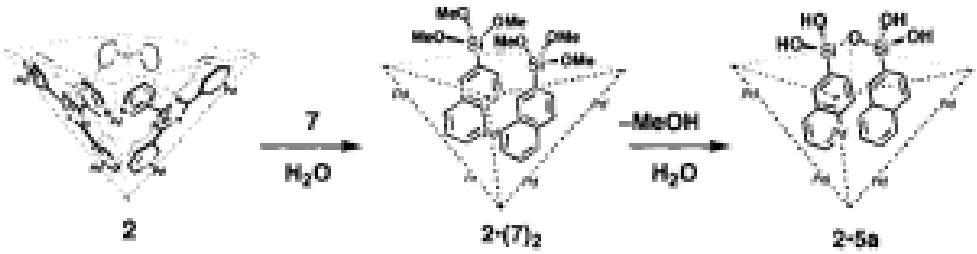
7
H_2O
-MeOH
H_2O
2
2·(7)$_2$
2·5a

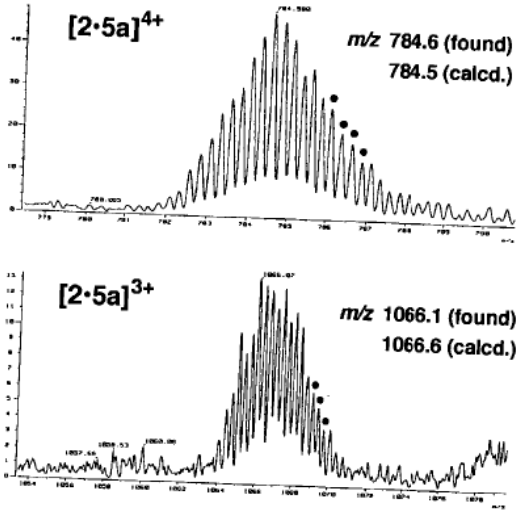
$[2\cdot5a]^{4+}$
m/z 784.6 (found)
784.5 (calcd.)
$[2\cdot5a]^{3+}$
m/z 1066.1 (found)
1066.6 (calcd.)

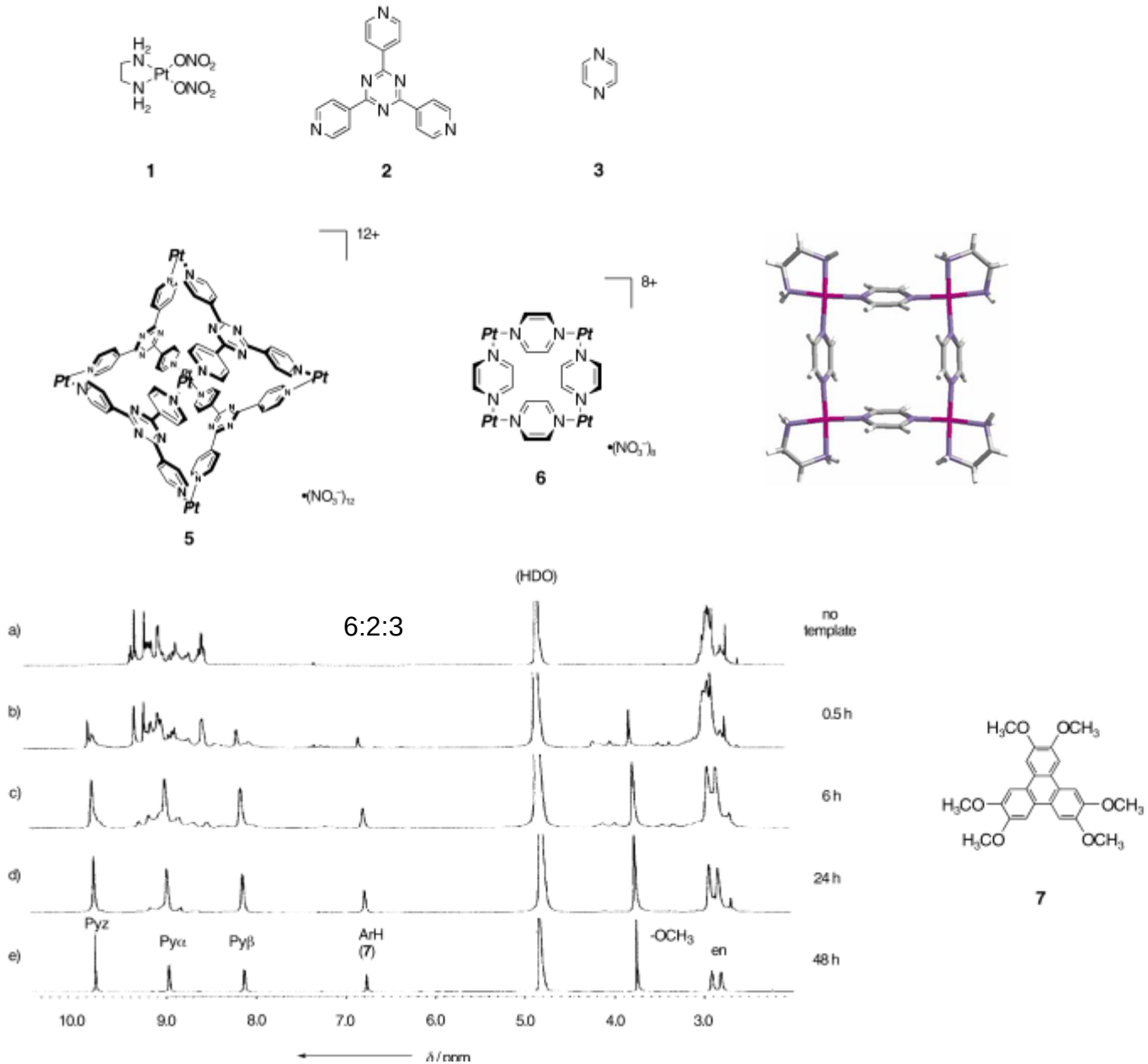

Figure 1. ^{1}H NMR spectra showing the guest-templated assembly of **7**⊂**4** complex (500 MHz, D_2O, 25 °C). a) A mixture of **1**, **2**, and **3**. Template **7** was added to this solution and the mixture was heated at 100 °C for b) 0.5 h, c) 6 h, d) 24 h, and e) 48 h. Pyz = pyrazine.

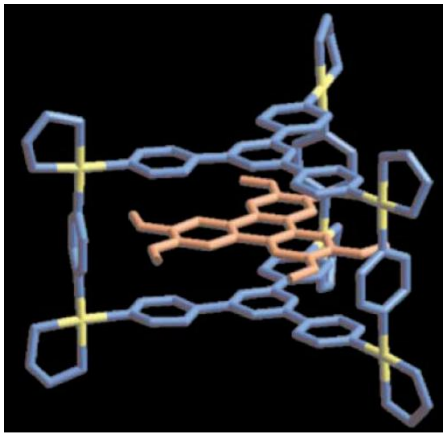

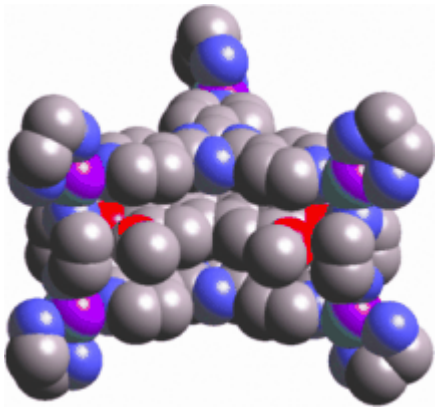

Fotodimerizzazioni 2+2

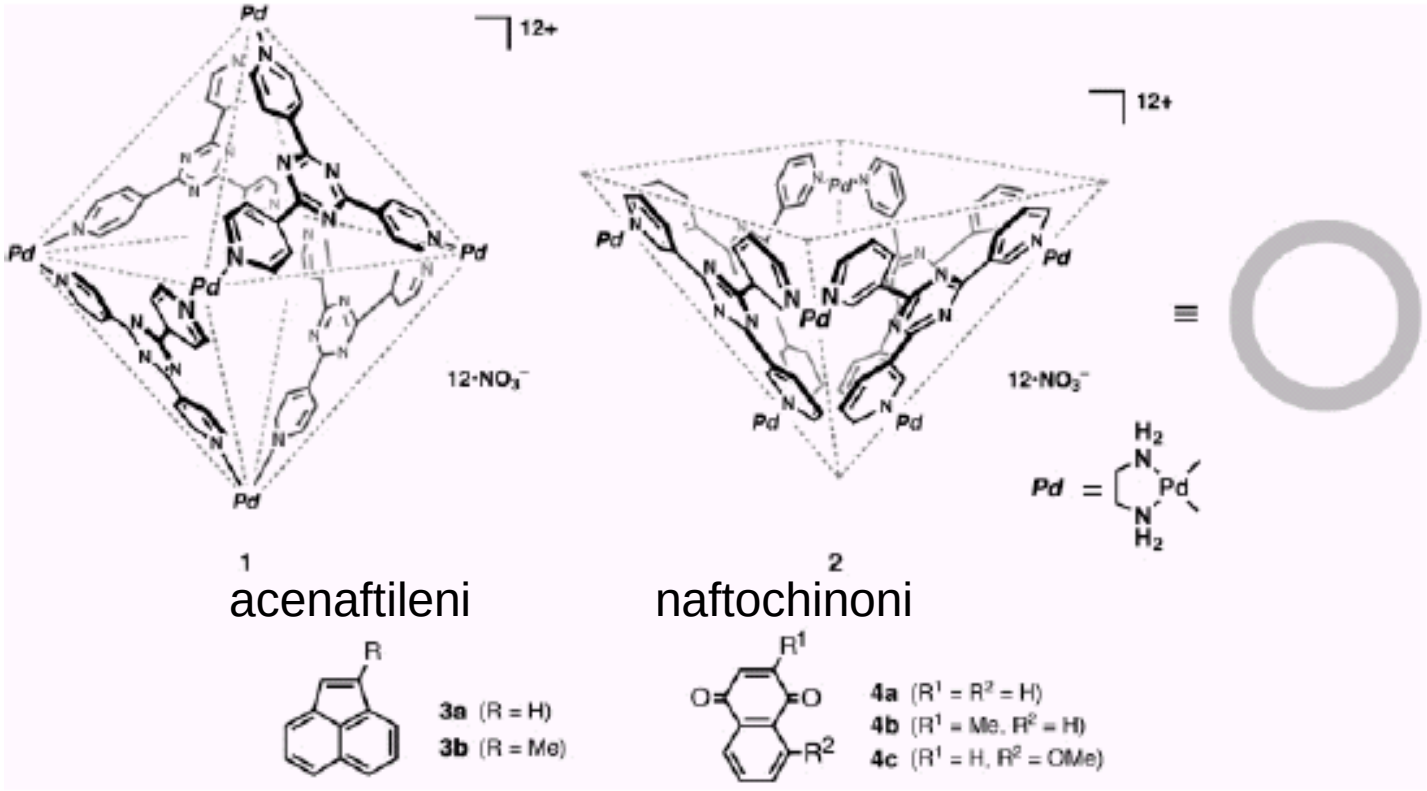

acenaftilene

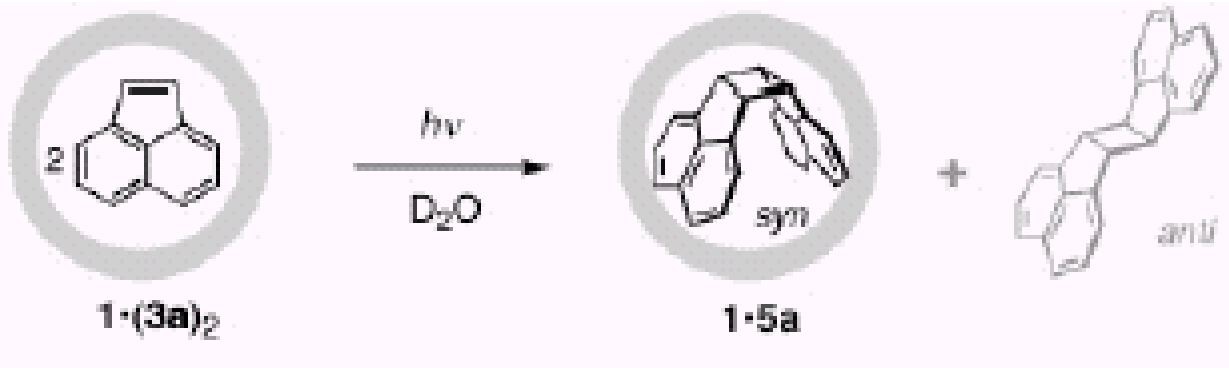

controllo stereochimica, [ ] 2mM resa > 98%

benzene: [ ] 150mM, 3h, resa 40%, no stereoselettività

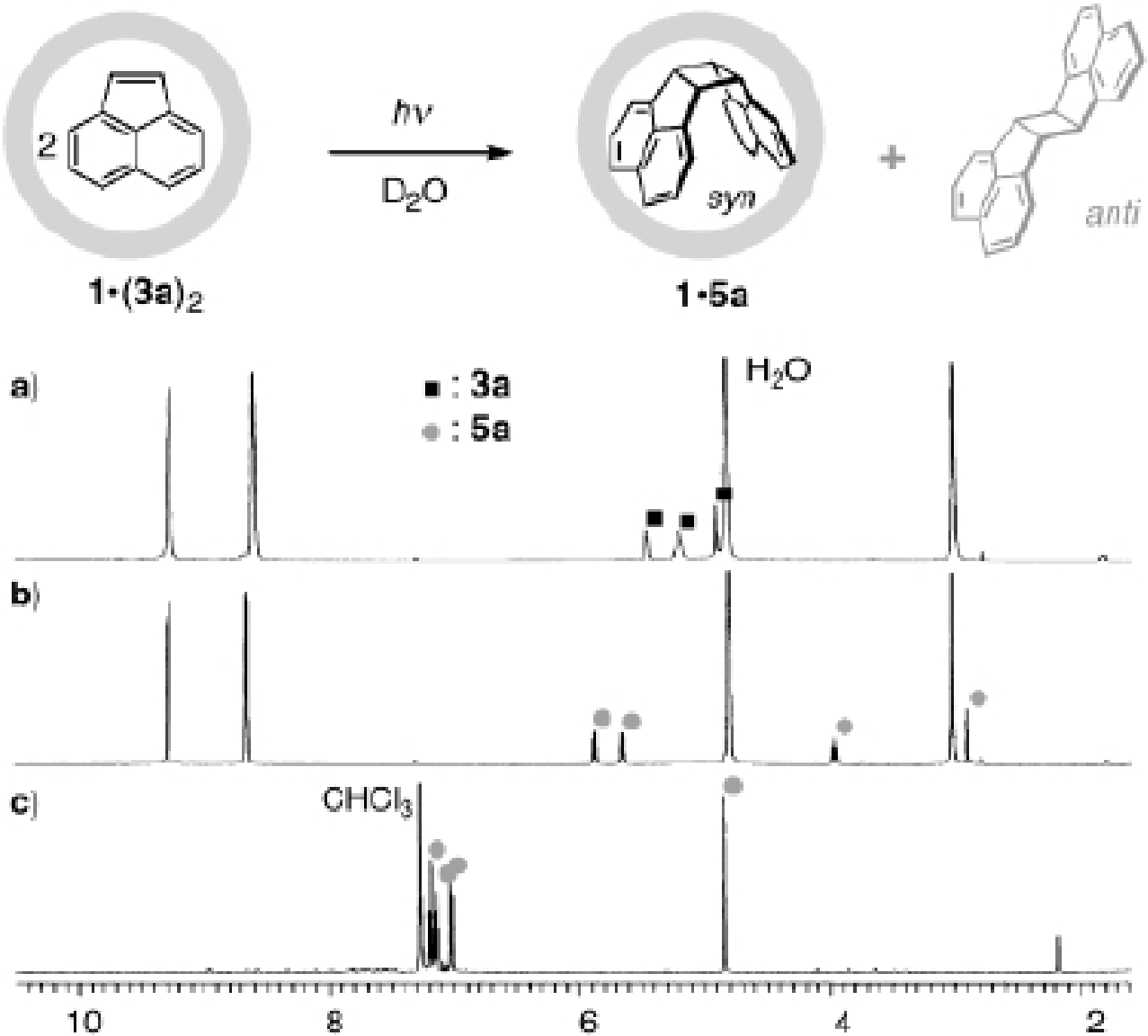

Figure 1. ^{1}H NMR spectroscopic analysis (500 MHz, D_2O, 27 °C) of the photodimerization of **3a** within cage **1:** a) before irradiation ($\mathbf{1}\cdot(\mathbf{3a})_2$) in D_2O; b) after irradiation (400 W) for 0.5 h; c) after extraction with $CDCl_3$.

1-metil-acenaftilene

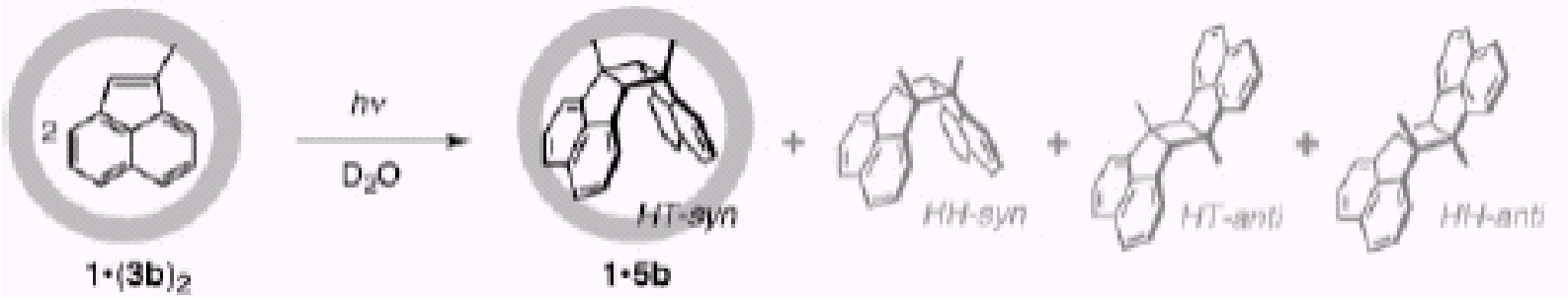

Controllo regiochimica, [ ] 2mM resa > 98%

naftochinone

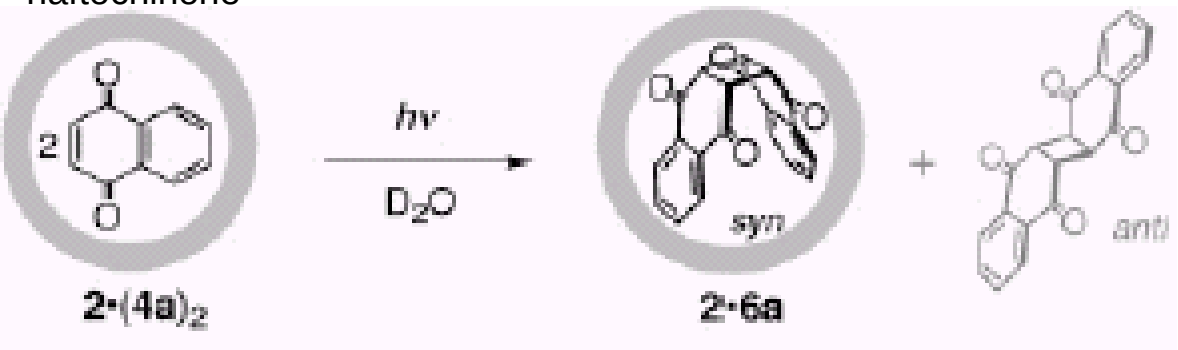

controllo stereochimica, [ ] 2mM resa > 98%

benzene: [ ] > >, t > >, resa 25%, 21% *anti*

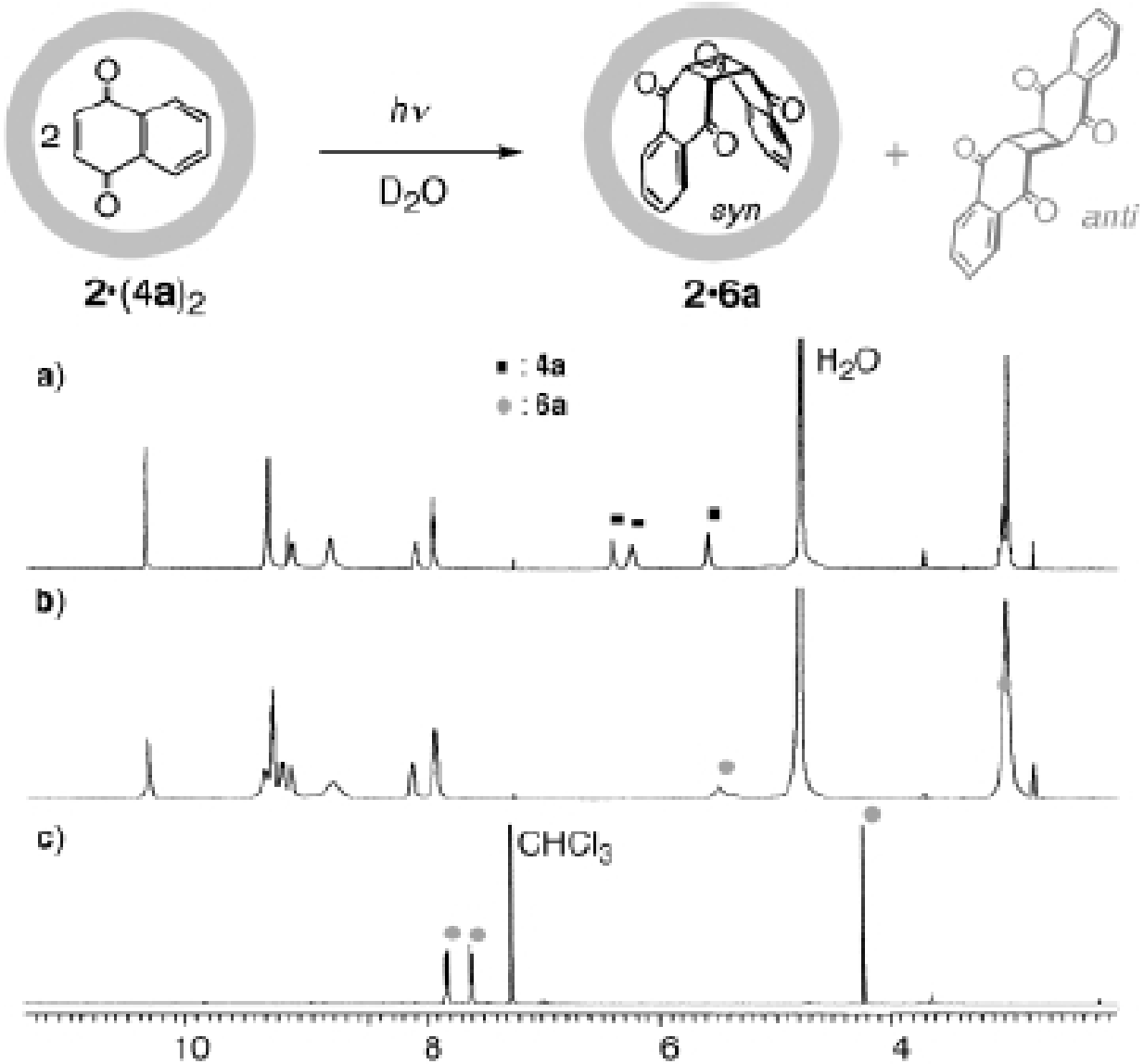

Figure 2. ^{1}H NMR spectroscopic analysis (500 MHz, D_2O, 27 °C) of the photodimerization of **4a** within bowl **2**: a) before reaction (**2**·(**4a**)$_2$) in D_2O; b) after irradiation (400 W) for 3 h; c) after extraction with $CDCl_3$.

Fig. 1. Self-assembled coordination cages (1 and 2), which are prepared by simple mixing of an exo-tridentate organic ligand and an end-capped Pd(II) ion in a 4:6 ratio in water.

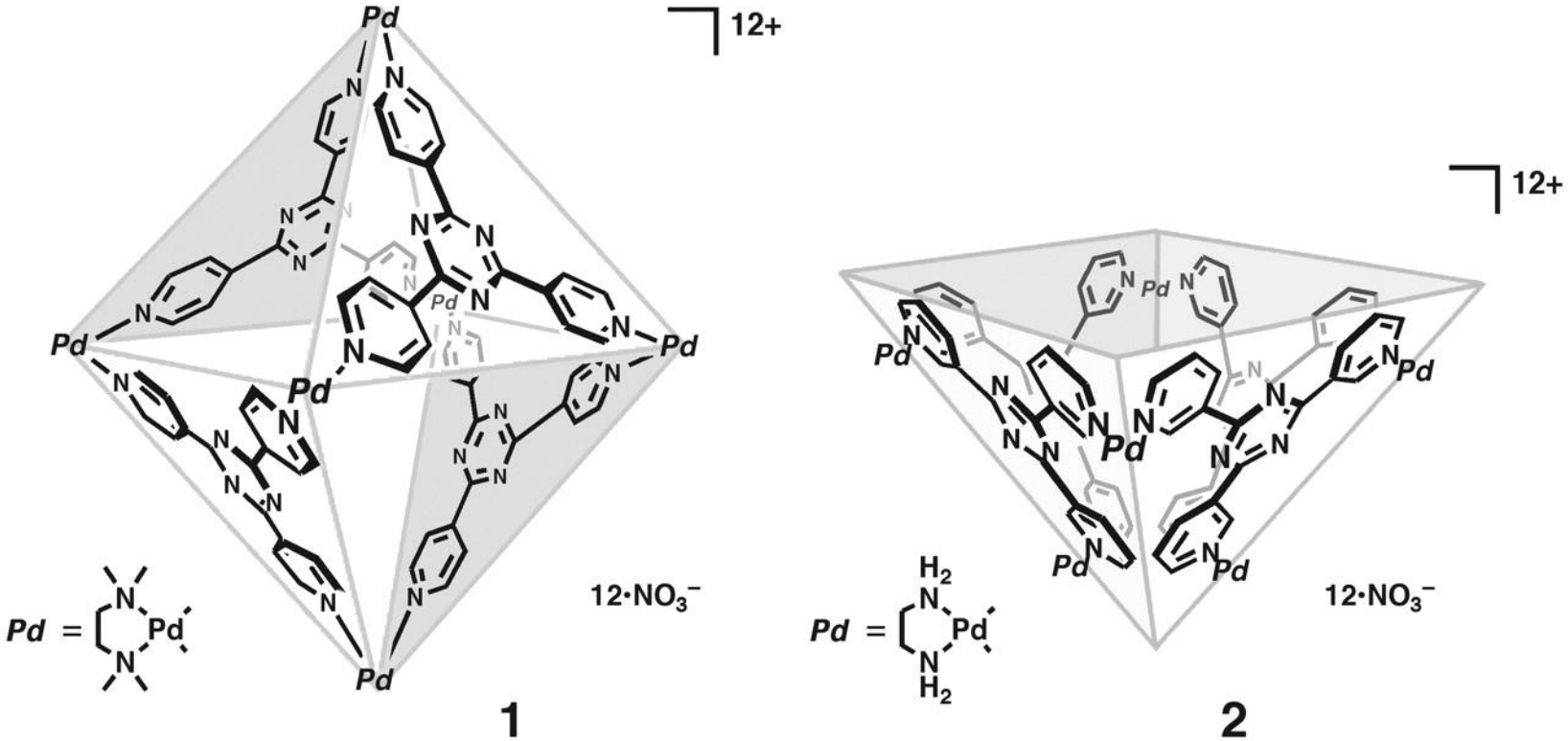

Michito Yoshizawa et al. Science 2006;312:251-254

Fig. 2. (A) Pair-selective encapsulation of two types of reactants, 9-hydroxymethylanthrancene (3a) andN-cyclohexylphthalimide (4a), within cage 1 and the subsequent Diels-Alder reaction leading to syn isomer of 1,4-adduct 5 within the cavity of 1

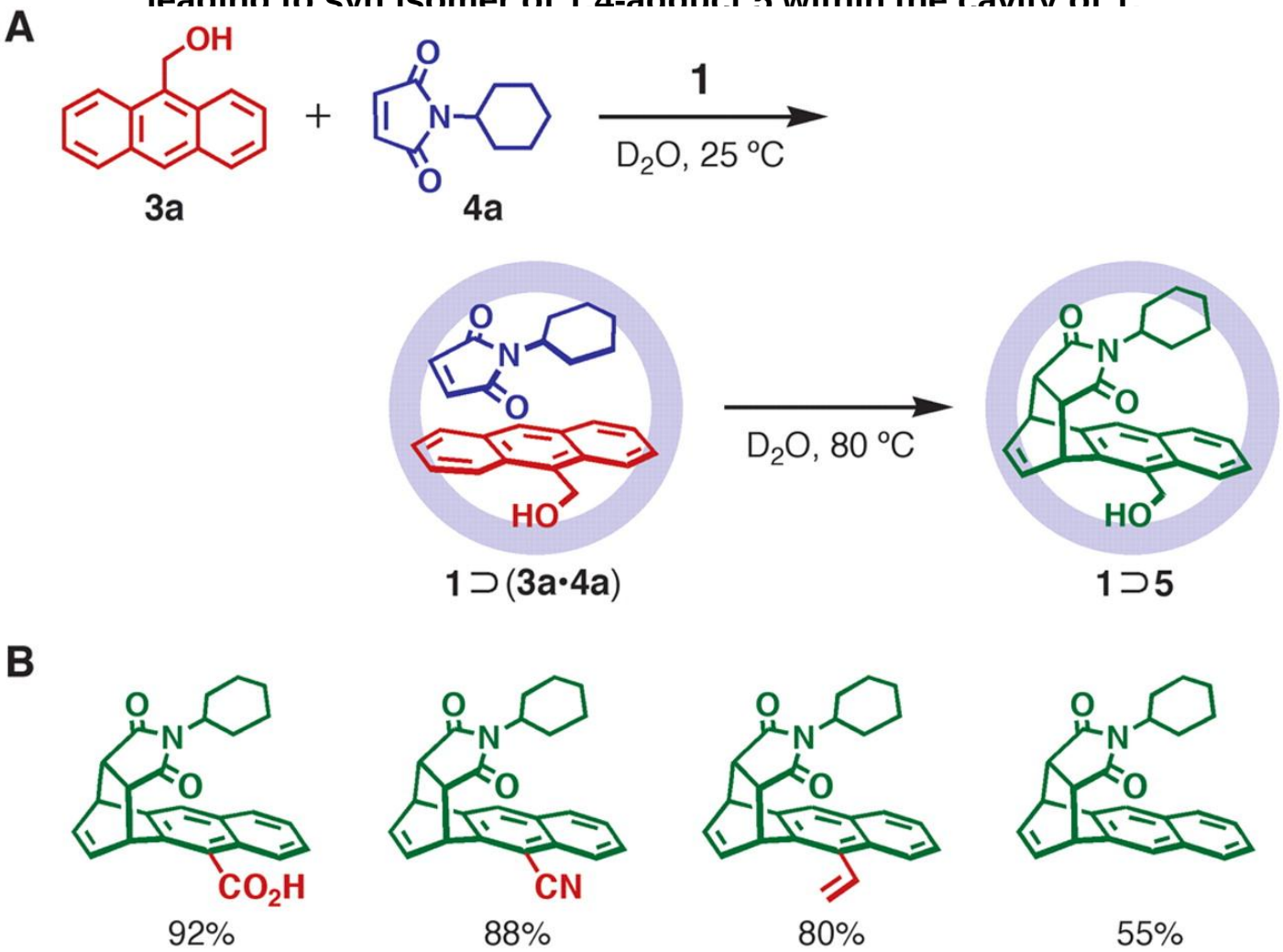

Michito Yoshizawa et al. Science 2006;312:251-254

Fig. 3. (A) Crystal structure of \batchmode \documentclass[fleqn,10pt,legalpaper]{article} \usepackage{amssymb} \usepackage{amsfonts} \usepackage{amsmath} \pagestyle{empty} \begin{document} \(\mathbf{1}{\supset}\mathbf{5}\) \end{document} 5 and (B) optimized structure of \batchmode \documentclass[fleqn,10pt,legalpaper]{article} \usepackage{amssymb} \usepackage{amsfonts} \usepackage{amsmath} \pagestyle{empty} \begin{document}

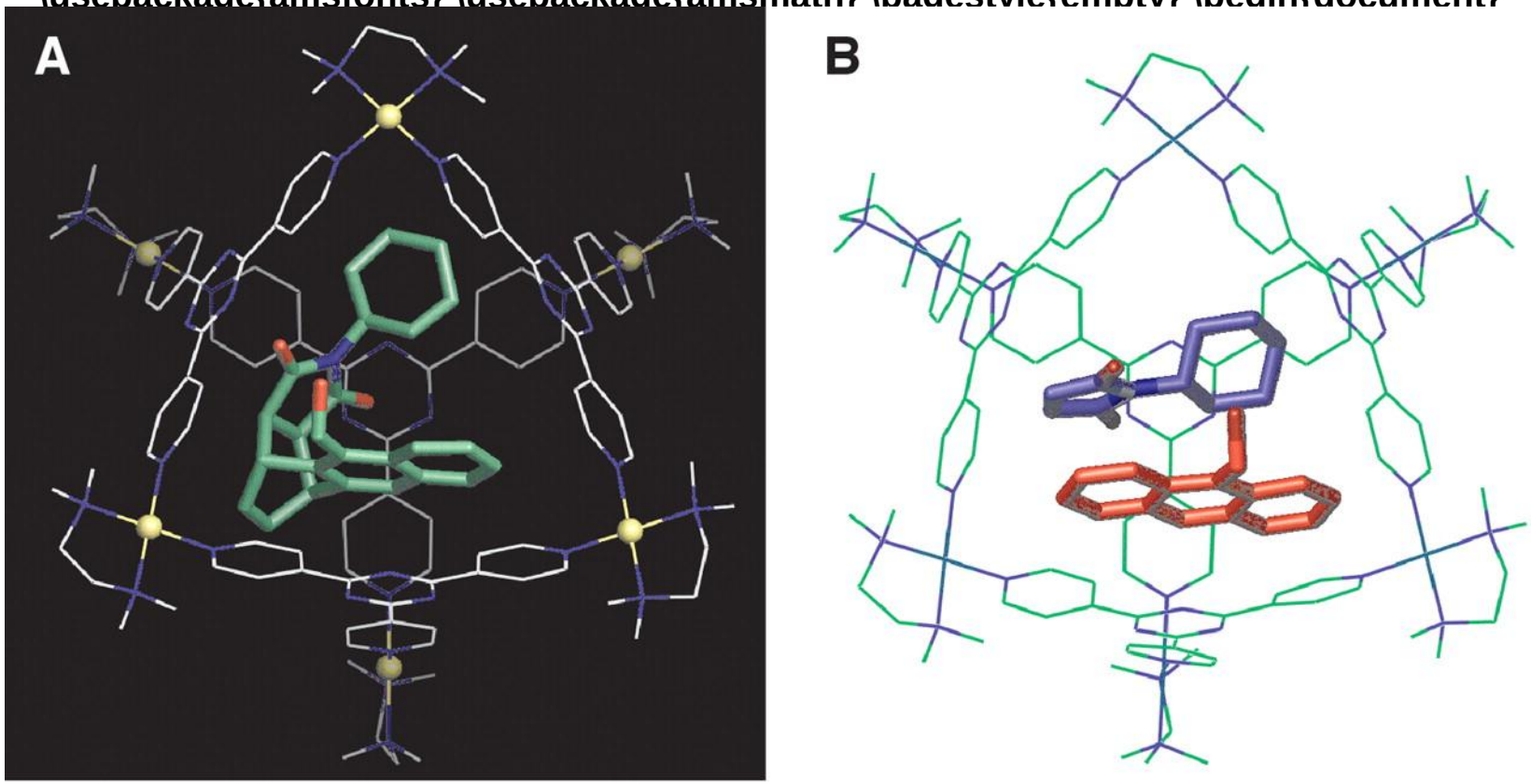

Michito Yoshizawa et al. Science 2006;312:251-254

Fig. 4. Catalytic Diels-Alder reaction of 9-hydroxymethylanthracene (3a) and N-phenylphthalimide (4c) in the aqueous solution of bowl 2, leading to 9,10-adduct 6.

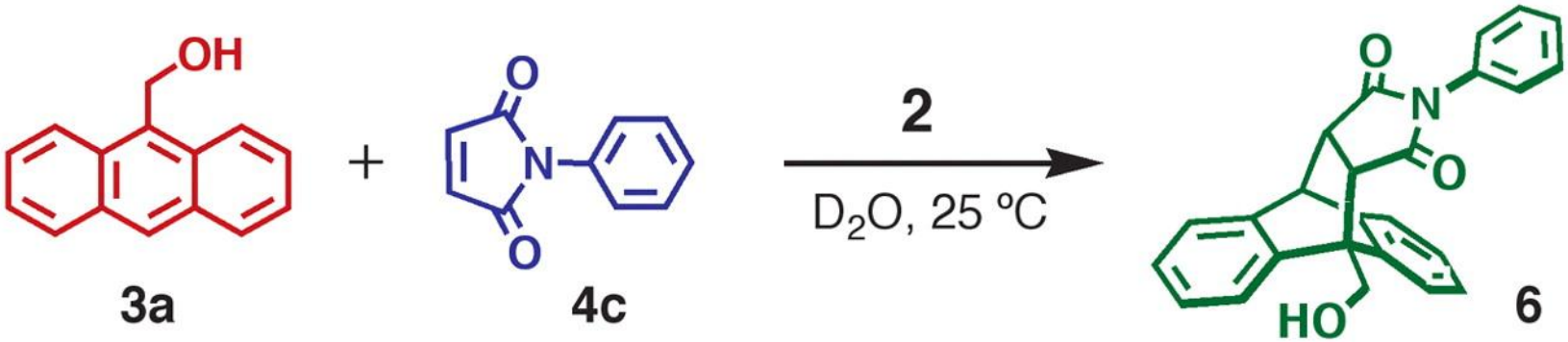

Michito Yoshizawa et al. Science 2006;312:251-254

Fig. 5. The 1H NMR spectra (500 MHz, room temperature) of the catalytic Diels-Alder reaction of 9-hydroxymethylanthrancene (3a) and N-phenylphthalimide (4c) in an aqueous solution of bowl 2

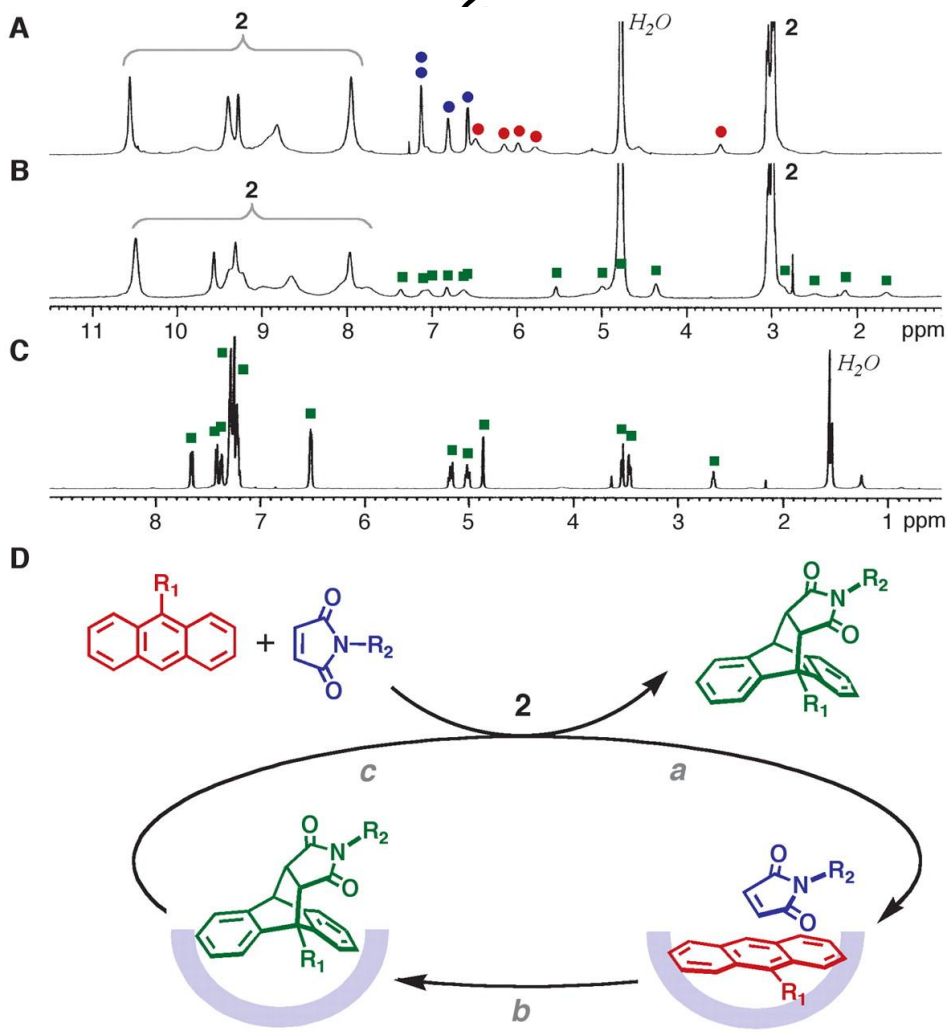

Michito Yoshizawa et al. Science 2006;312:251-254

Table S1. Catalytic Diels-Alder reaction of **3** and **4** in the presence of **2** (10 mol%) in H_2O (1 mL) and control experiments in H_2O or $CDCl_3$ (1 mL) without **2**.

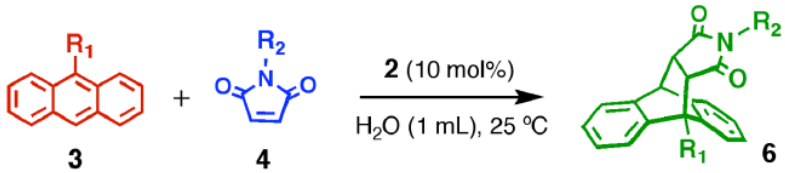

Entry	Substrate		Time	Yield(%) of **6**		
	3 (R_1)	**4** (R_2)		with **2**	without **2**	in $CHCl_3$[†]
1	$-CH_2OH$	propyl	5 h	>99	8	0
2	$-CH_2OH$	cyclohexyl	15 h	98	0	6
3	$-CH_2OH$	phenyl	5 h	>99[*,†]	3	9
4	$-CH_2OH$	phenyl	15 h	6	7	21
5	$-CH_2OH$	benzyl	5 h	>99	trace	0
6	$-CH_2OH$	xylyl	15 h	94	0	17
7	$-CH_3$	cyclohexyl	7 h	>99	0	5
8	$-CH_3$	phenyl	3 h	>99	5	17
9	$-CH{=}CH_2$	phenyl	1 d	88	0	trace
10	$-CH{=}CH_2$	benzyl	1 d	97	5	4
11	$-CO_2H$	benzyl	1 d	12	0	0
12	$-CH_2OH$	phenyl	1 d	>99[‡]	—	—

[*] $(en)Pd(NO_3)_2$: 10 mol% [†] without **2** [‡] **2** : 1 mol%, hexane (1 mL)

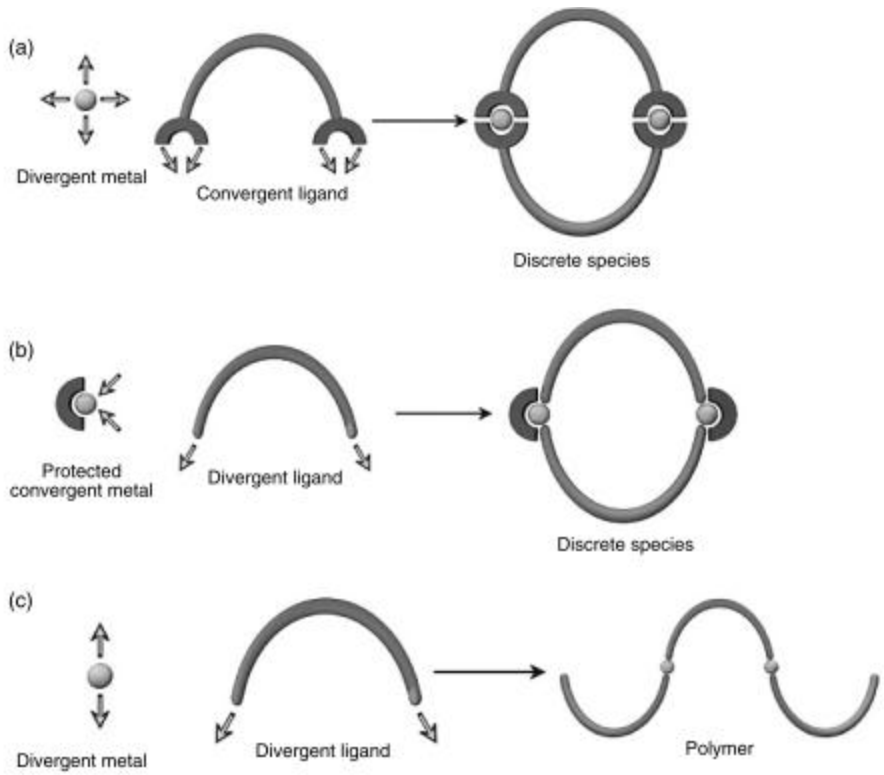
(a)
Divergent metal
Convergent ligand
Discrete species
(b)
Protected
convergent metal
Divergent ligand
Discrete species
(c)
Divergent metal
Divergent ligand
Polymer

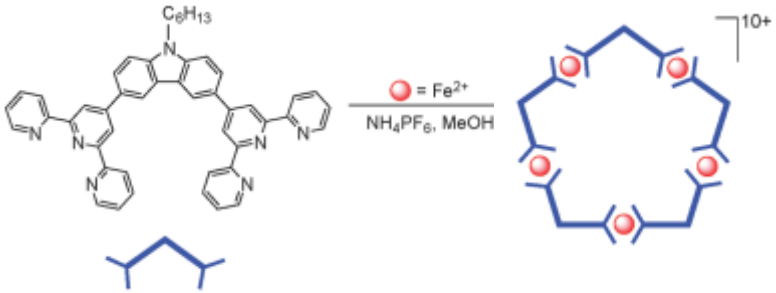
C6H13
N
N
N
N
N
N
N
N
= Fe2+
NH4PF6, MeOH
10+

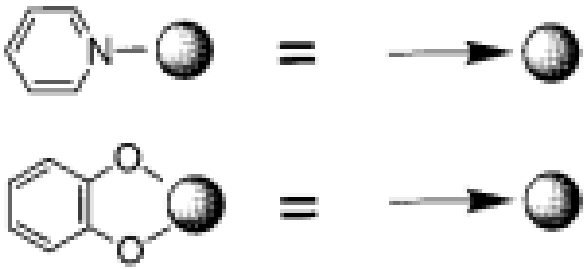
N
=
O
O
=

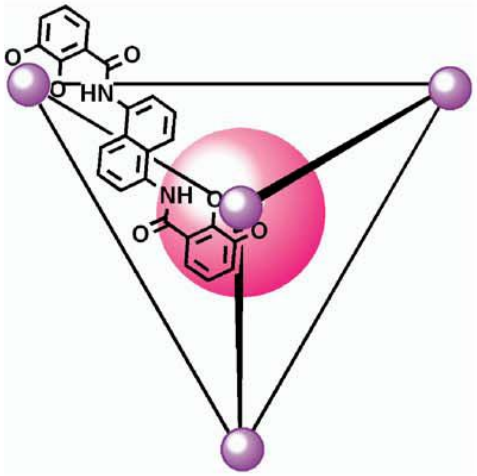

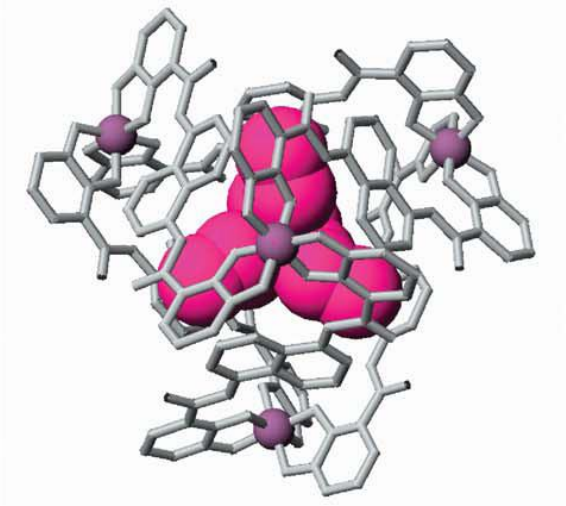

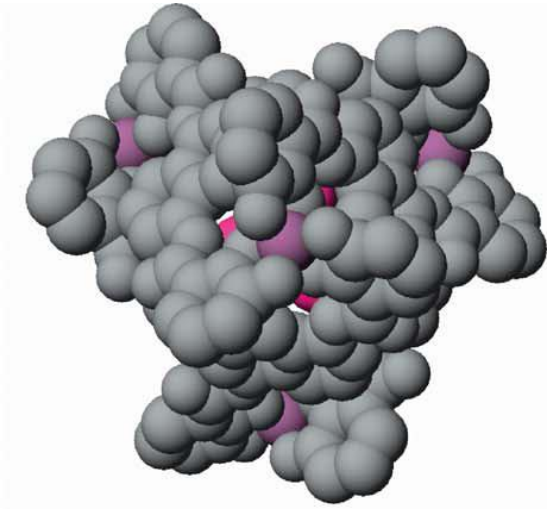

M_4L_6, (Ga^{3+}, Fe^{3+}; biscatecol-amidi) 12^-, ΔΔΔΔ, ΛΛΛΛ, 300-350 Å
Stabilizzazione di cationi organici

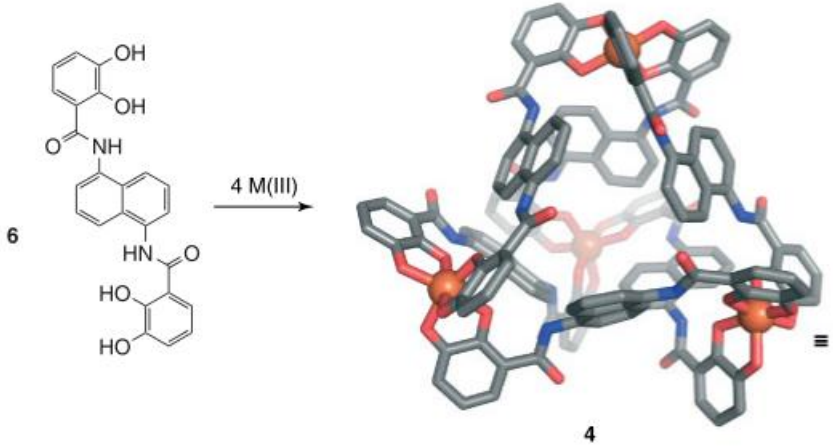

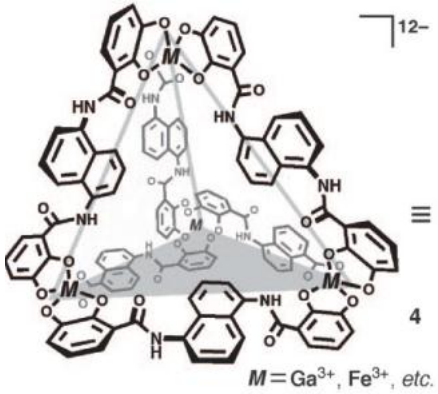

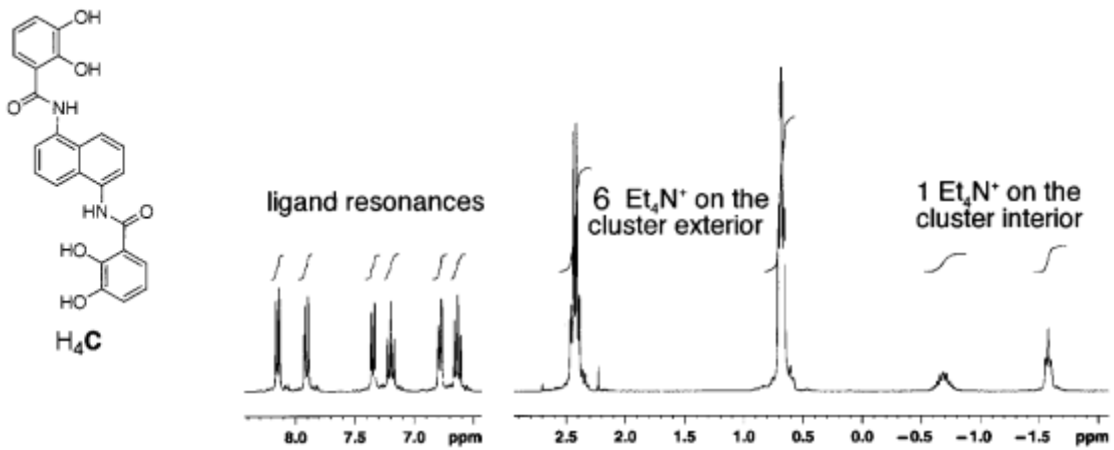

Figure 14. ^{1}H NMR (D_2O) depicting the two sets of Et_4N^+ resonances characteristic of the exterior and encapsulated cations.

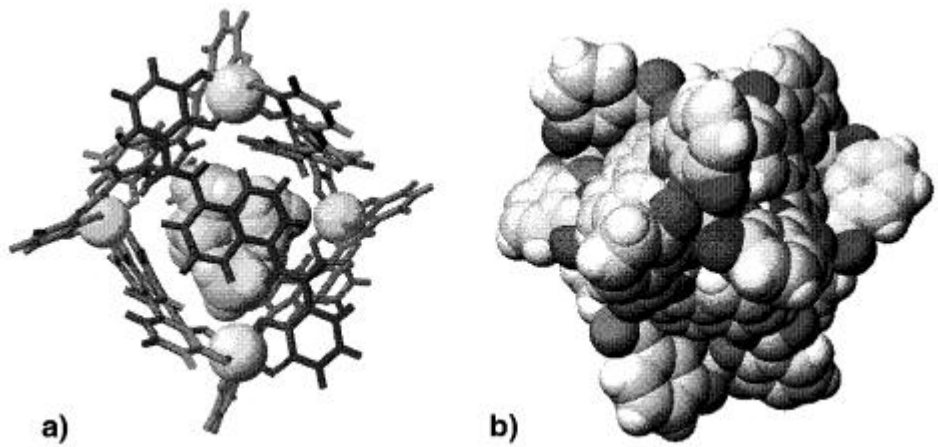

Figure 15. Based on the X-ray structure coordinates, $Et_4N^+ \subset [Fe_4C_6]^{12-}$ in both (a) wire-frame and (b) space-filling representations.

(B)

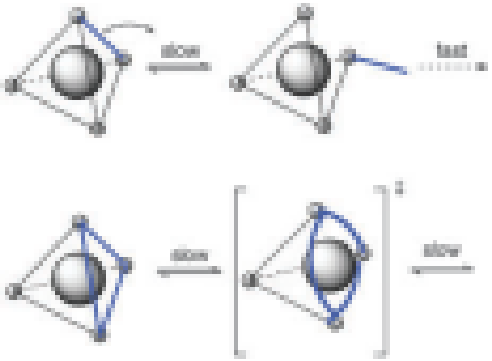

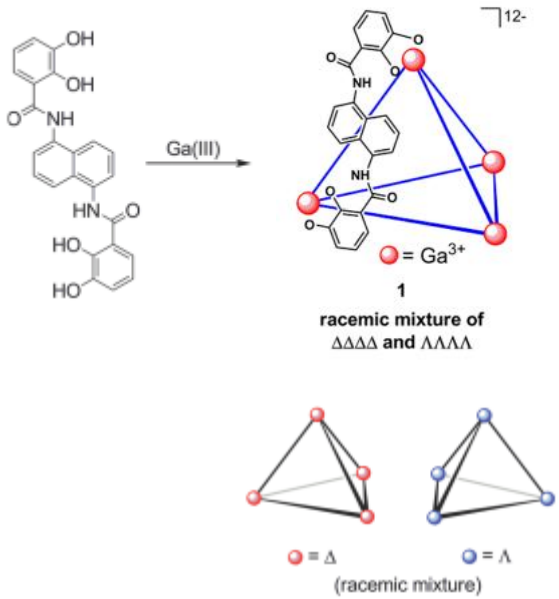

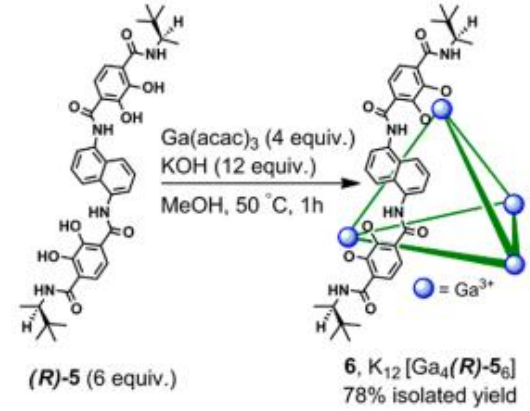

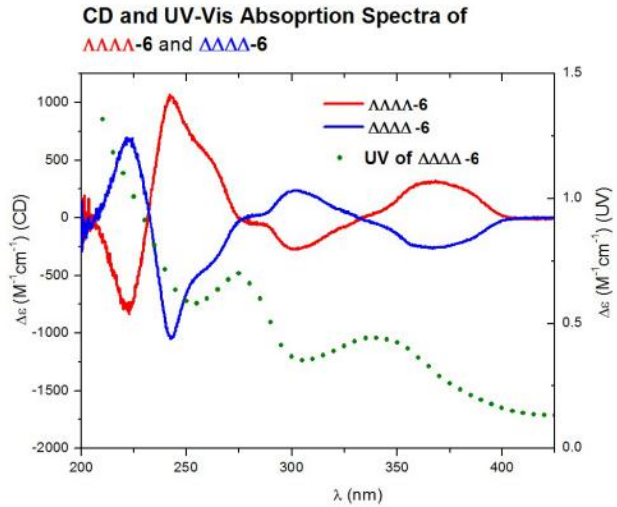

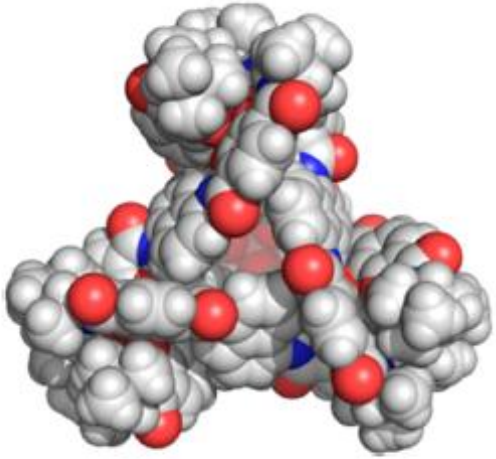

Figure 2. X-ray structure of ΔΔΔΔ-6.

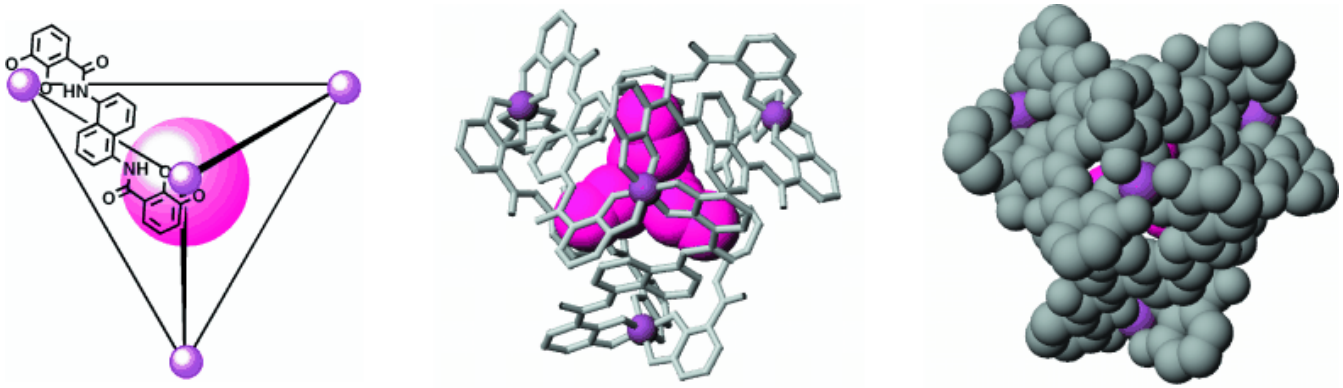

Left: A schematic view of the [G⊂M_4L_6] (G=guest) supramolecular tetrahedral assembly, looking down the C_3-axis. For clarity only one ligand is drawn, the other ligands are represented as sticks. Middle: CAChe model of [NPr_4⊂Fe_4L_6]$^{11-}$, the guest molecule is shown in a space-filling view, the hydrogen atoms are omitted for clarity. Right: The same CAChe model as in the middle, now with host and guest in space filling view. This representation shows that the guest molecule is not exposed to the assembly exterior, but rather is tightly surrounded by the host.

Supramolecular Catalysis of a Unimolecular Transformation: Aza-Cope Rearrangement within a Self-Assembled Host, Volume: 43, Issue: 48, Pages: 6748-6751, First published: 08 December 2004, DOI: (10.1002/anie.200461776)

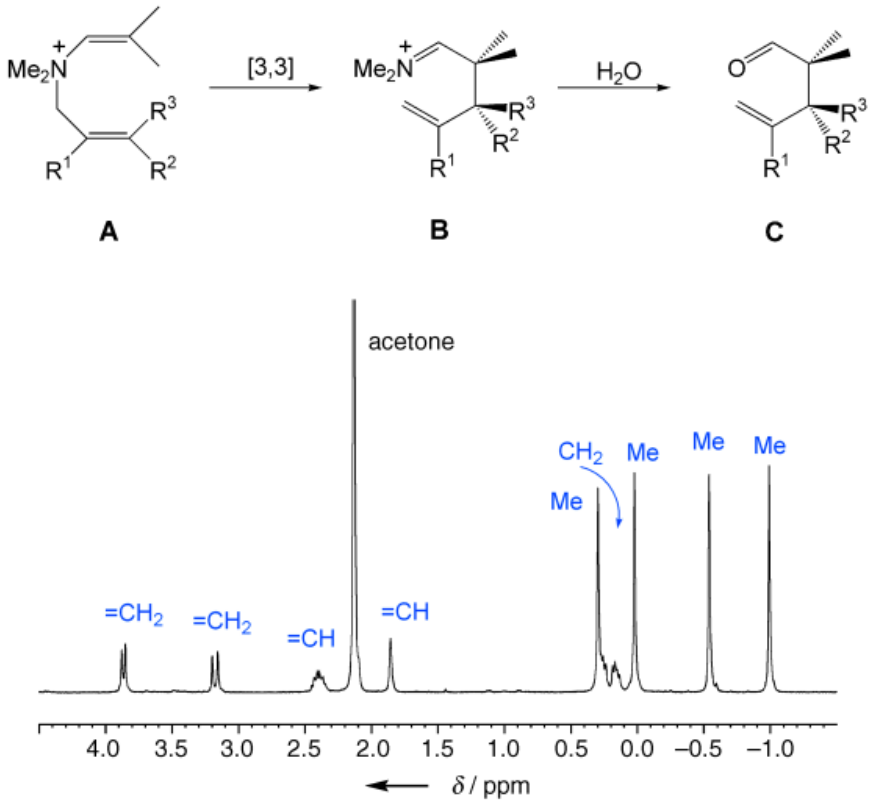

Top: A general reaction scheme of the 3-aza-Cope rearrangement. Starting from the enammonium cation **A**, [3,3] sigmatropic rearrangement leads to iminium cation **B**, which then hydrolyzes to the aldehyde, **C**. Bottom: ^{1}H NMR spectrum of [**1**⊂Ga_4L_6]$^{11-}$ (**1**: R^1, R^2, R^3=H). The observed upfield shift of guest resonance signals illustrates the close contact between host and guest.

Supramolecular Catalysis of a Unimolecular Transformation: Aza-Cope Rearrangement within a Self-Assembled Host, Volume: 43, Issue: 48, Pages: 6748-6751, First published: 08 December 2004, DOI: (10.1002/anie.200461776)

Table 1. Rate constants for free (k_{free}) and encapsulated (k_{encaps}) rearrangements (measured at 50 °C) and their acceleration factors.

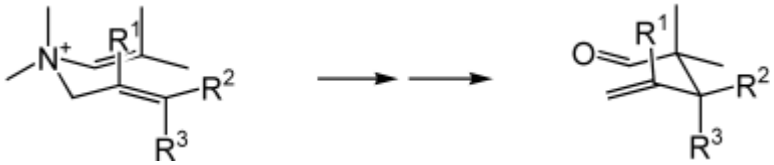

Substrate	R^1	R^2	R^3	k_{free} [$\times 10^{-5}$ s^{-1}]	k_{encaps} [$\times 10^{-5}$ s^{-1}]	Acceleration
1	H	H	H	3.49	16.3	5
2	Me	H	H	7.61	198	26
3	H	Et	H	3.17	446	141
4	H	H	Et	1.50	135	90
5	H	*n*Pr	H	4.04	604	150
6	H	H	*n*Pr	1.69	74.2	44
7	H	*i*Pr	H	0.37	316	854

Supramolecular Catalysis of a Unimolecular Transformation: Aza-Cope Rearrangement within a Self-Assembled Host, Volume: 43, Issue: 48, Pages: 6748-6751, First published: 08 December 2004, DOI: (10.1002/anie.200461776)

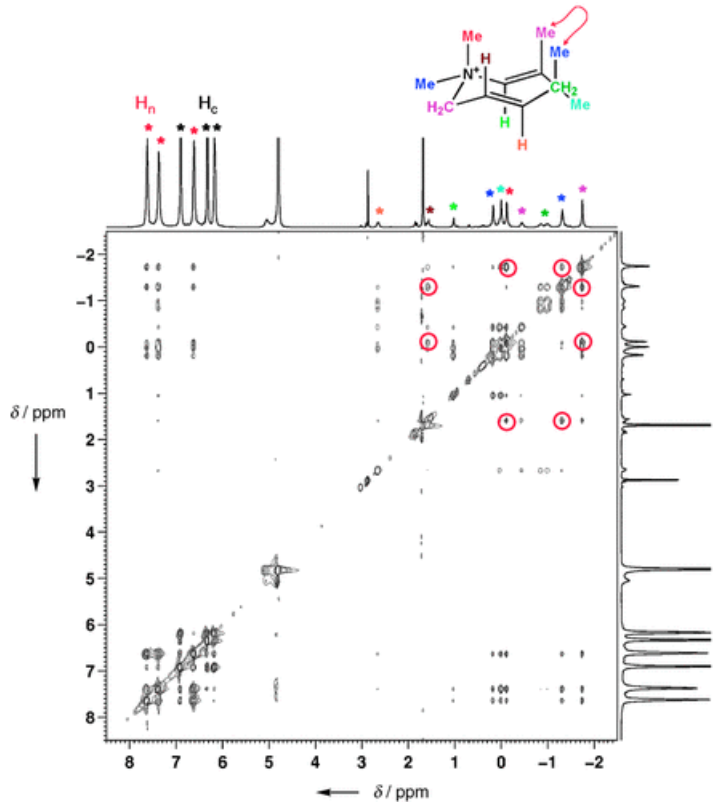

The 2D NOESY spectrum of [**3**⊂Ga_4L_6]$^{11-}$ in a D_2O/MeOD mixture (70:30) recorded at −10 °C, mixing time 100 ms. Indicated in red are selected NOEs. The correlation between Me and Me at the two distal ends of the molecule demonstrates the cavity's enforcement of a compressed and folded guest conformation. H_n=naphthyl protons, H_c=catechol protons.

Supramolecular Catalysis of a Unimolecular Transformation: Aza-Cope Rearrangement within a Self-Assembled Host, Volume: 43, Issue: 48, Pages: 6748-6751, First published: 08 December 2004, DOI: (10.1002/anie.200461776)

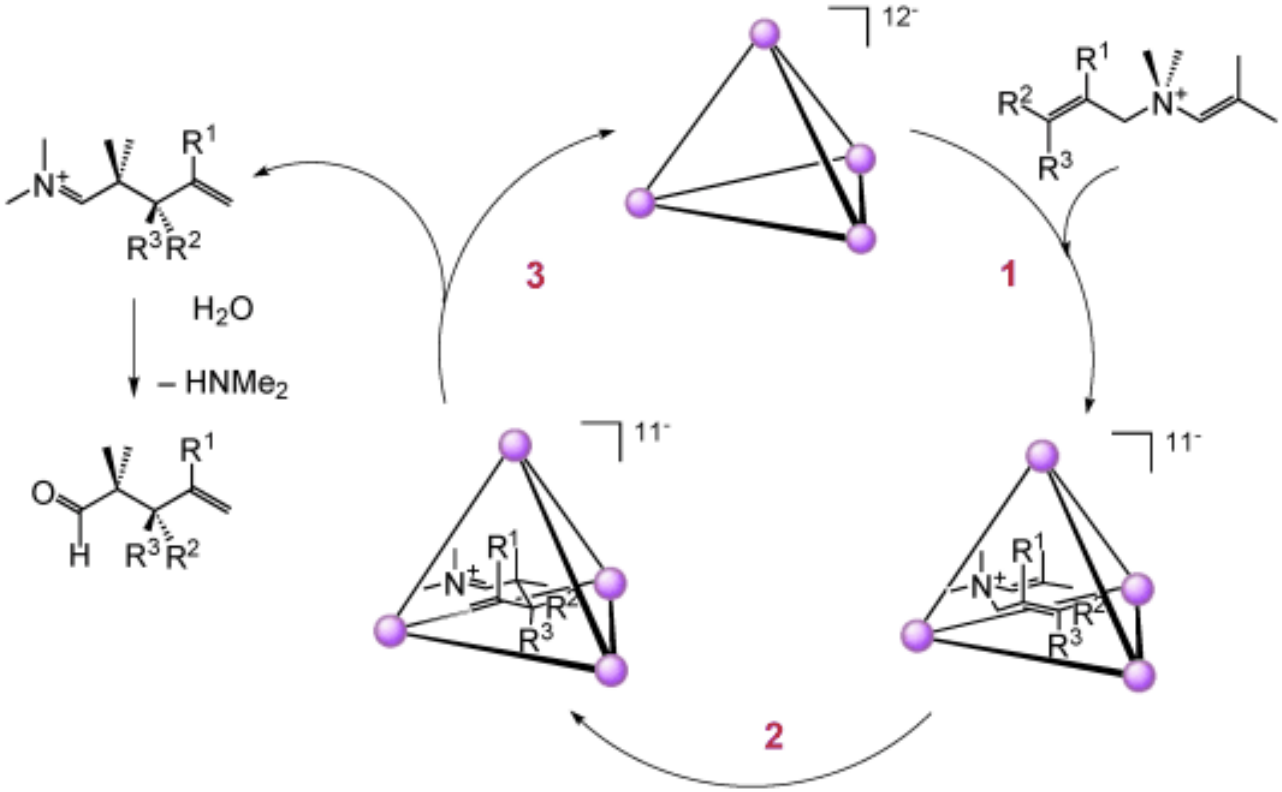

Proposed catalytic cycle for the cationic 3-aza-Cope rearrangement, see text for details.

Supramolecular Catalysis of a Unimolecular Transformation: Aza-Cope Rearrangement within a Self-Assembled Host, Volume: 43, Issue: 48, Pages: 6748-6751, First published: 08 December 2004, DOI: (10.1002/anie.200461776)

Acid Catalysis in Basic Solution: A Supramolecular Host Promotes Orthoformate Hydrolysis

Michael D. Pluth, *et al.*

Science **316**, 85 (2007);
DOI: 10.1126/science.1138748

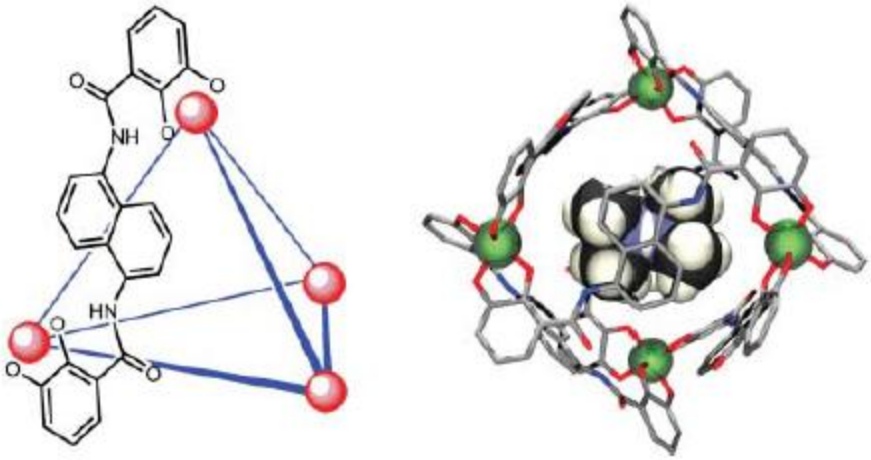

Fig. 1. (**Left**) A schematic representation of the host M_4L_6 assembly. Only one ligand is shown for clarity. (**Right**) A model of $[\mathbf{2}\text{-}H^+ \subset \mathbf{1}]^{11-}$; hydrogen atoms on the host assembly are omitted for clarity.

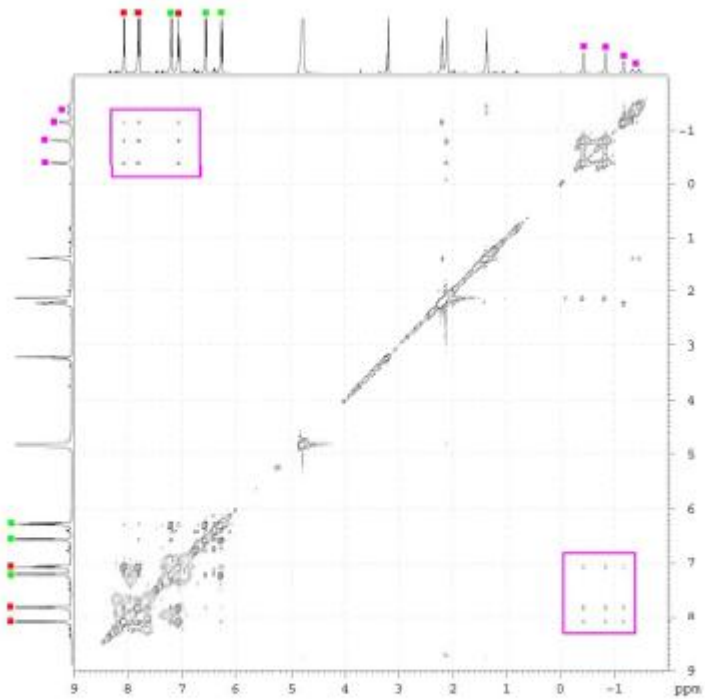

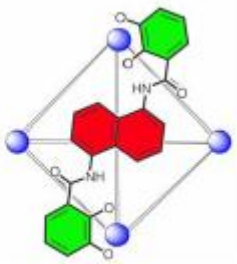

Figure S1 ^{1}H 2D NOESY of [**2**-H$^+$ ⊂ **1**]$^{11-}$ in D_2O, 22 °C, with 100 ms mixing time. The strong cross peaks between the naphthalene protons of **1** and the guest protons of **2**-H$^+$ show strong through-space correlation indicative of encapsulation.

spin H-P coupling constant ($^1J_{DP}$) = 75 Hz. In H_2O, the undecoupled ^{31}P NMR spectrum showed a doublet ($^1J_{HP}$ = 490 Hz) corresponding to a one-bond P-H coupling that definitively establishes binding of a proton to phosphorus.

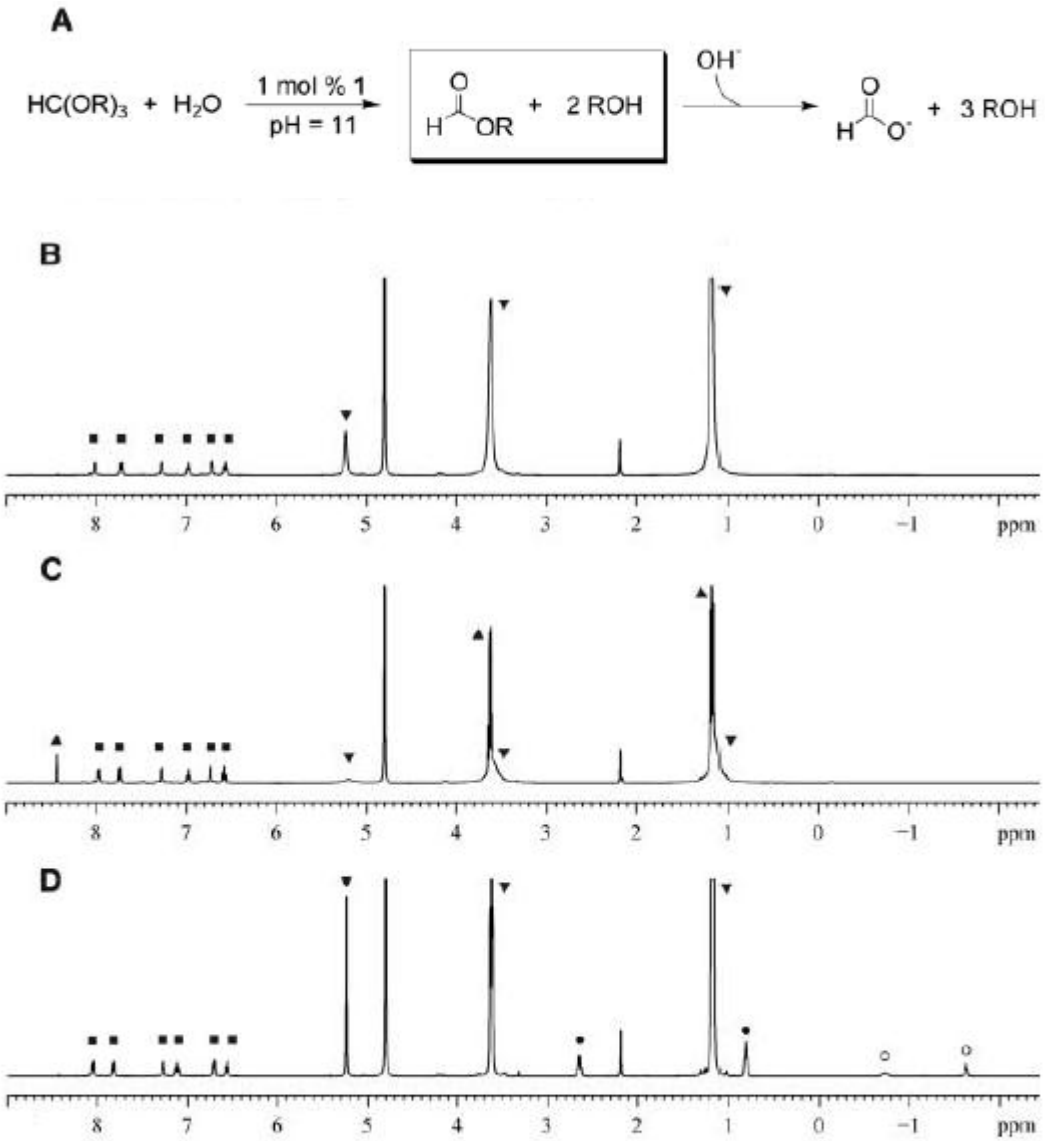

Fig. 2. (**A**) Reaction and substrate scope for orthoformate hydrolysis in the presence of catalytic **1**. Bu, butyl; Me, methyl; Pr, propyl. (**B** to **D**) All spectra taken with 50 equivalents (equiv.) of triethyl orthoformate with respect to **1** at pD = 11.0, 100 mM K_2CO_3, 22°C, in D_2O. (B) Initial spectrum. (C) Spectrum after 60 min. (D) Spectrum of **1** with 2 equiv. NEt_4^+ after 60 min. Molecule **1** represented by ■; $HC(OEt)_3$, ▼; NEt_4^+, ● for exterior and ○ for interior, and product HCO_2H, ▲.

reached. Although the pK_a of **3**-H^+ is 10.8 in free solution, stabilization of the protonated form by **1**, which can be calculated as the product of the pK_a and the binding constant of the protonated amine, shifts the effective basicity to 14.3 (*32*). This dramatic shift highlights the substantial stabilization of the protonated species over the neutral species upon encapsulation in the highly charged cavity (*33*).

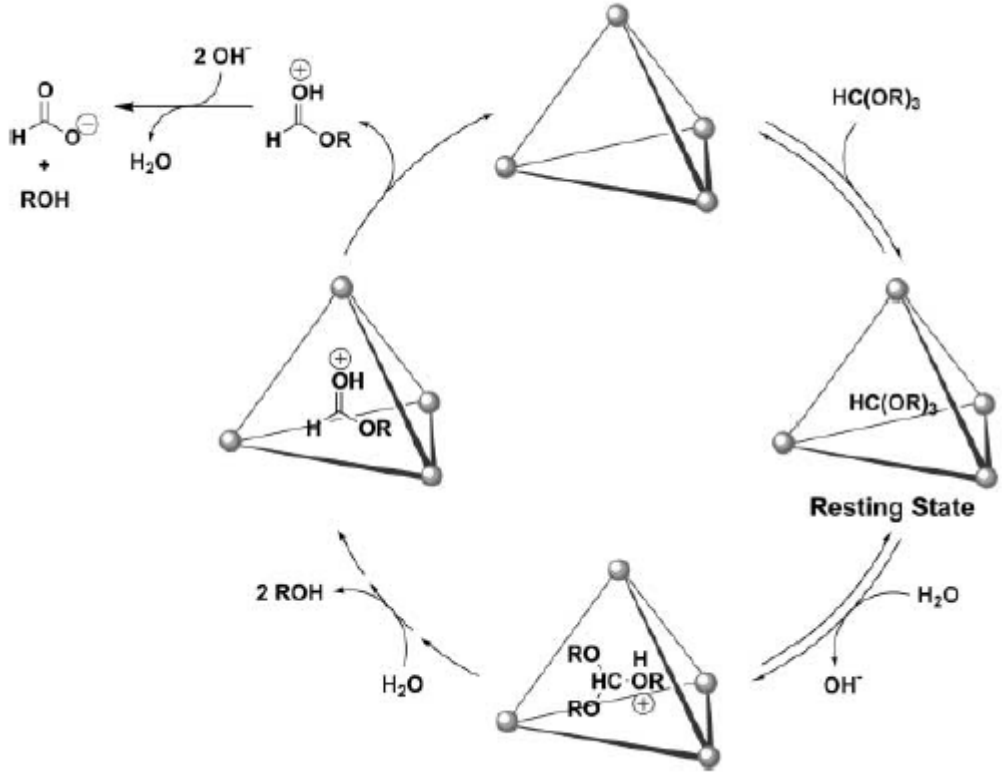

Fig. 3. Mechanism for catalytic orthoformate hydrolysis in the presence of catalytic **1**.

ChemComm

Chemical Communications

www.rsc.org/chemcomm

Volume 49 | Number 25 | 28 March 2013 | Pages 2465–2580

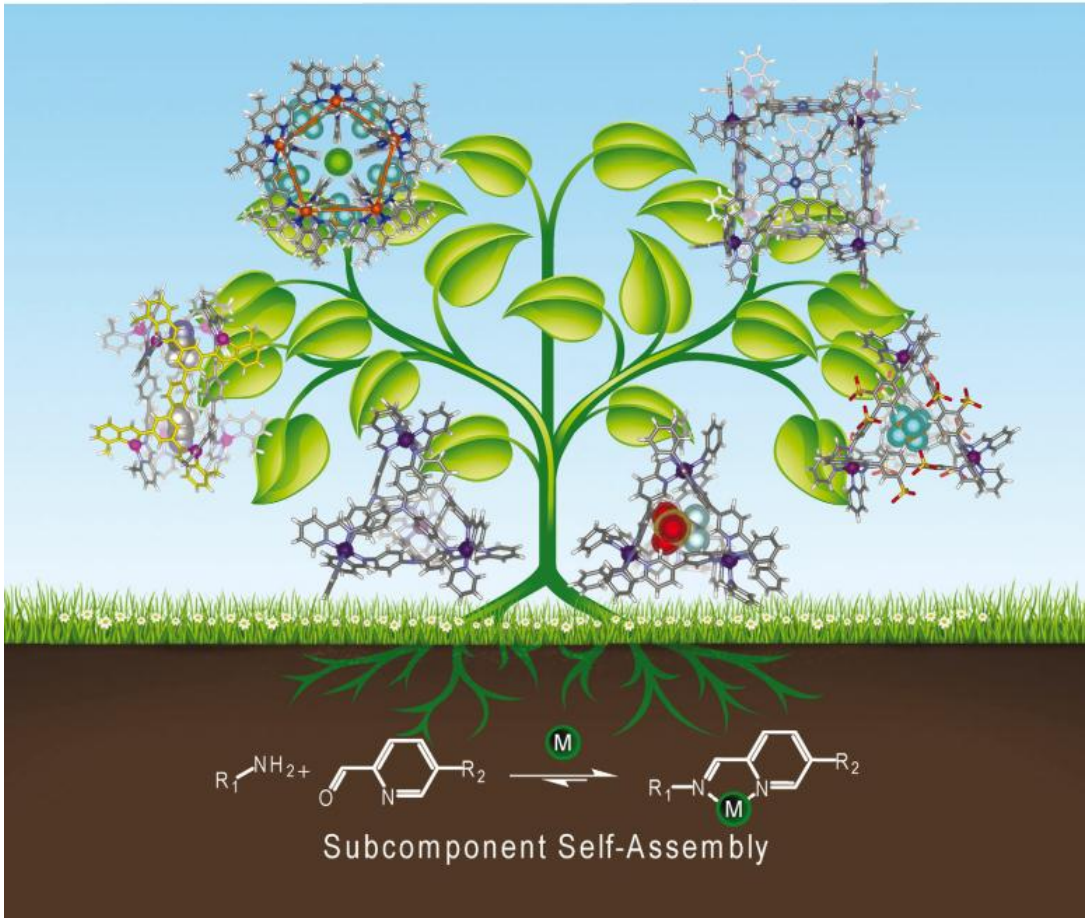

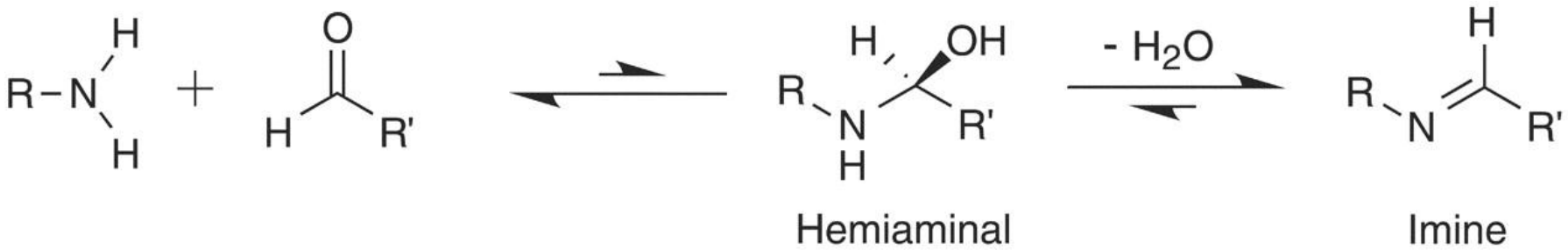
- H2O
Hemiaminal
Imine


12 Me4NOH
4 FeSO4.7H2O
H2O
6
12
1

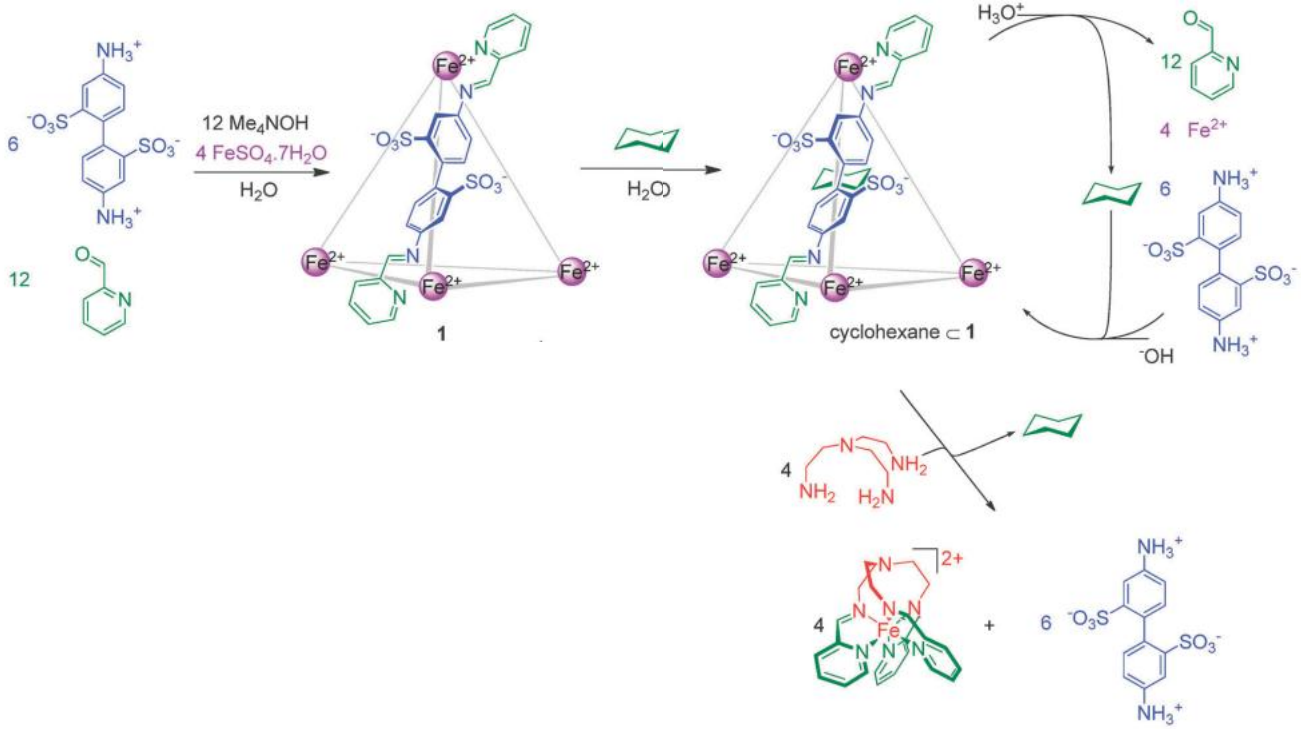
6
12
12 Me4NOH
4 FeSO4.7H2O
H2O
1
H2O
cyclohexane ⊂ 1
H3O+
12
4 Fe2+
6
-OH
4
+
6

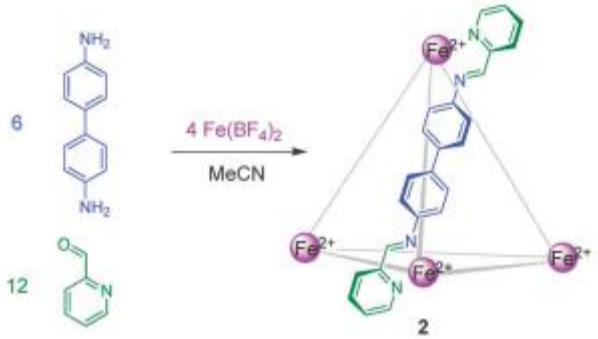
6
12
4 Fe(BF4)2
MeCN
2

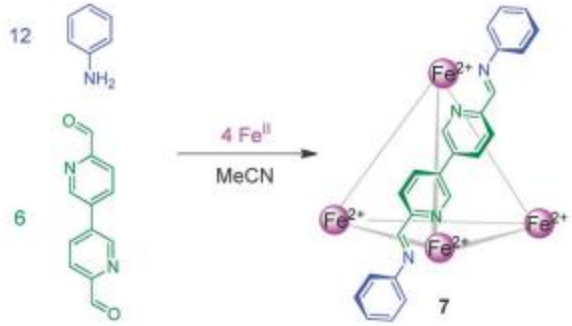
12
6
4 Fe^II
MeCN
7

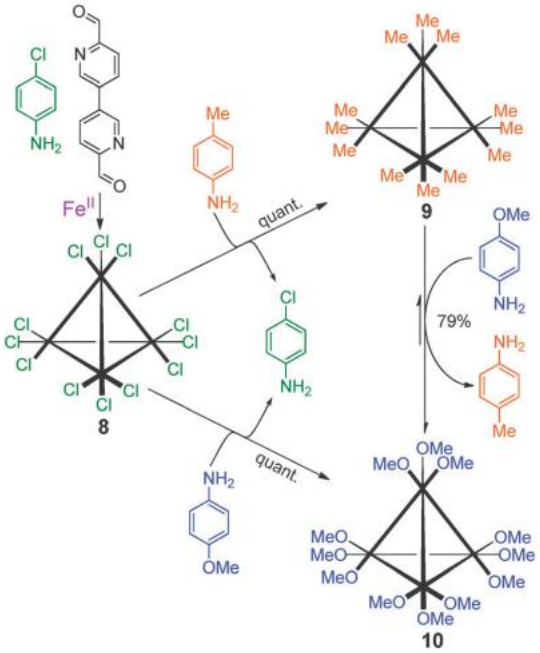
Fe^II
quant.
quant.
79%
8
9
10

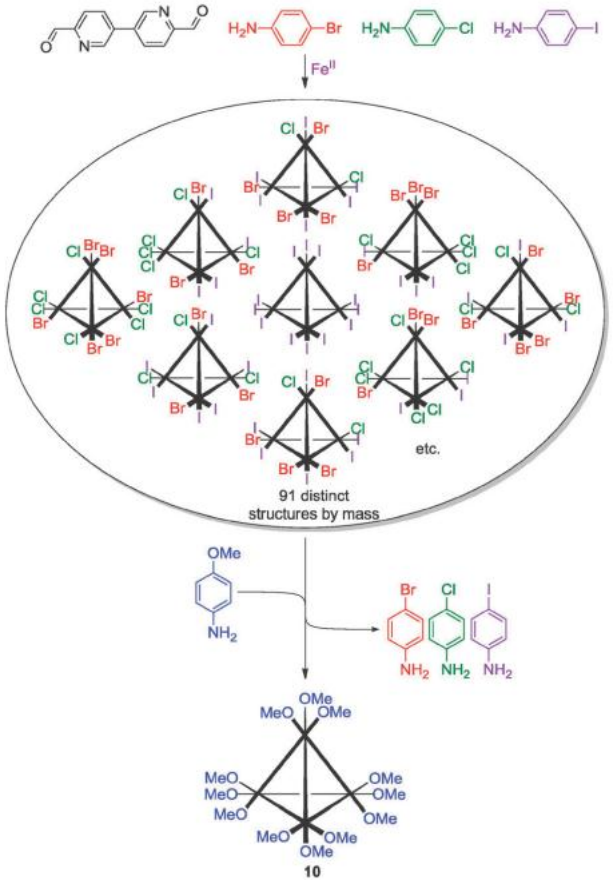
Fe^II
91 distinct
structures by mass
etc.
10

White Phosphorus Is Air-Stable Within a Self-Assembled Tetrahedral Capsule

Prasenjit Mal,[1] Boris Breiner,[1] Kari Rissanen,[2] Jonathan R. Nitschke[1*]

SCIENCE VOL 324 26 JUNE 2009

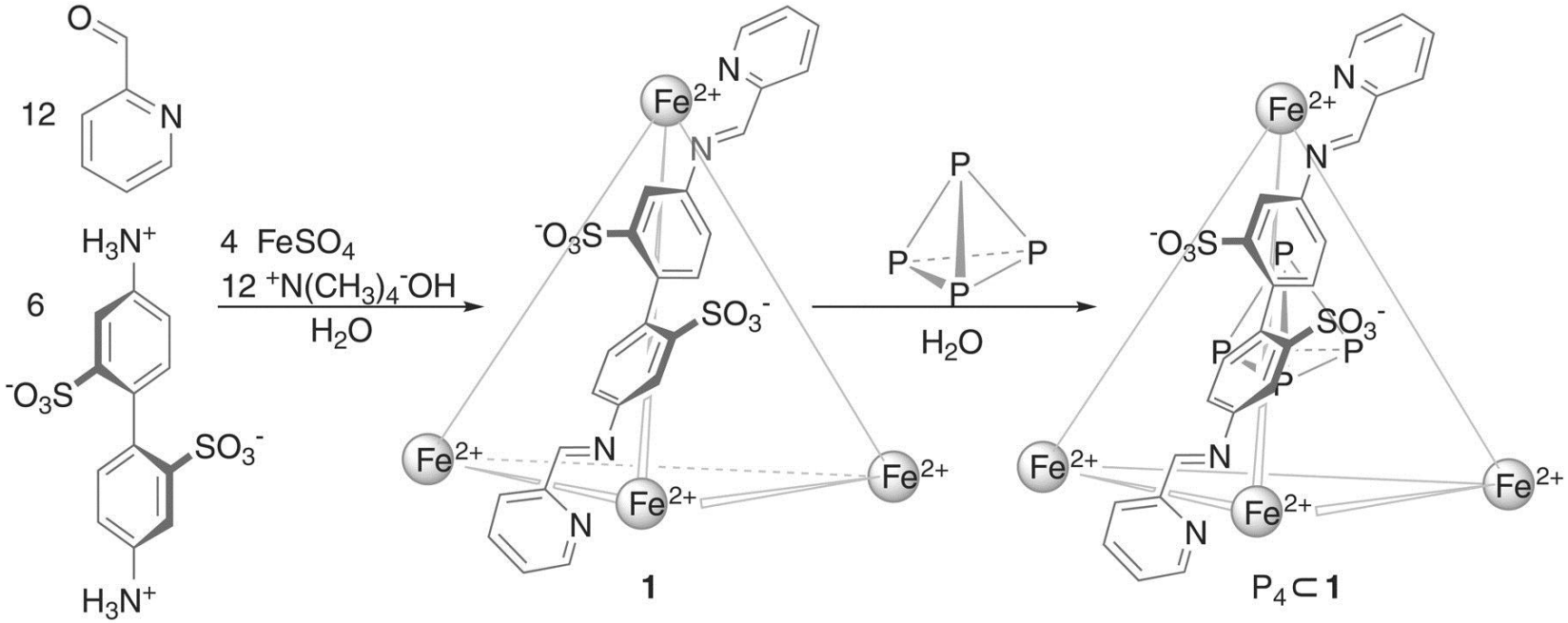

Fig. 1 Synthesis of tetrahedral cage 1 and subsequent incorporation of P4.

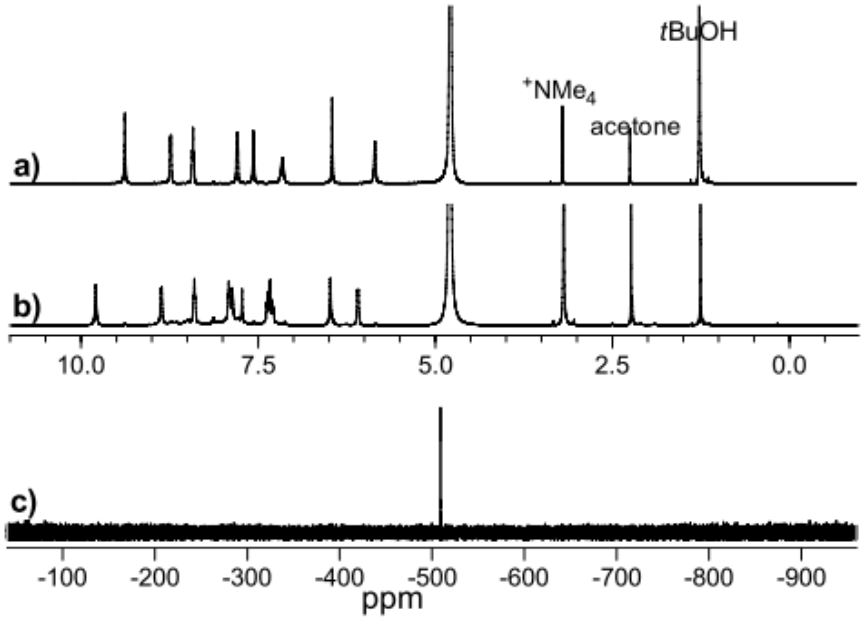

Figure S1. ^{1}H NMR spectra in D_2O of cage **1** (top), of $P_4 \subset$**1** (middle), and ^{31}P NMR spectrum of $P_4 \subset$**1** (bottom).

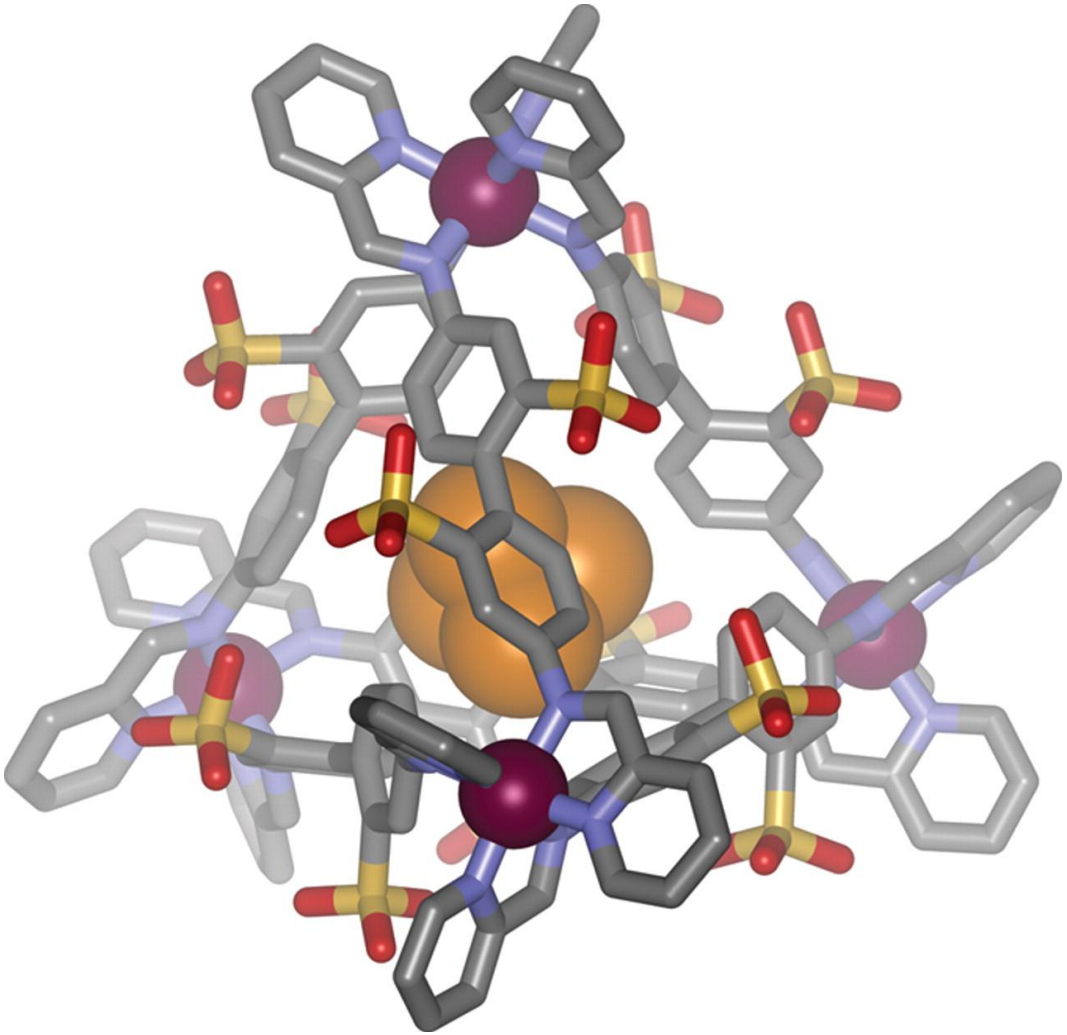

Fig. 2 Crystal structure of P4⊂1.

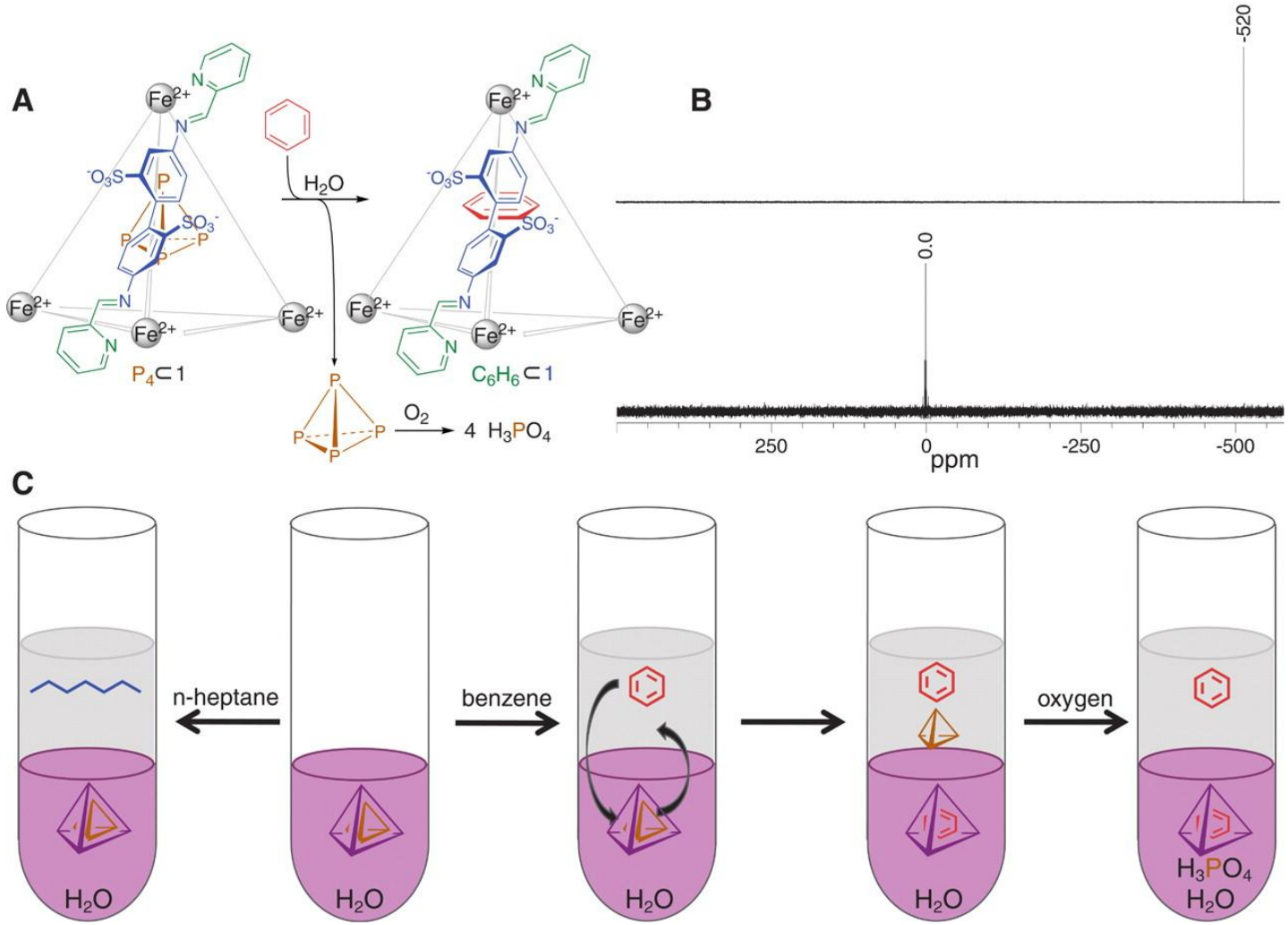

Fig. 3 Extraction of P4 from 1 by n-heptane is not possible, whereas replacing P4 with another suitable guest (benzene or cyclohexane) results in the facile removal of P4 into the organic solvent.

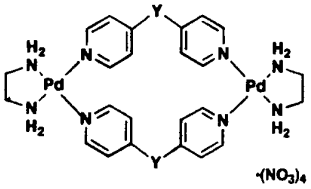
Y
Pd
N
H2
·(NO3)4

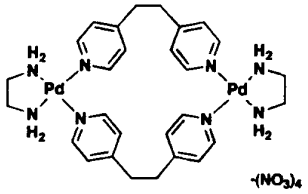
Pd
N
H2
·(NO3)4

Y = CH_2

Y = $C(OH)_2$

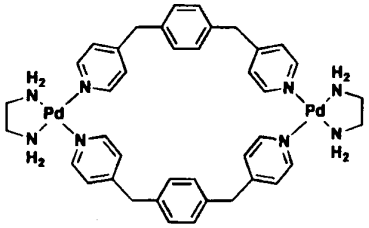
Pd
N
H2

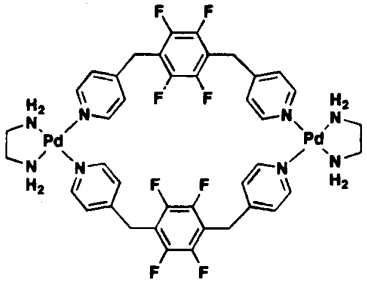
F
Pd
N
H2

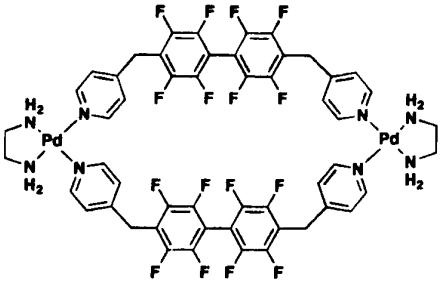
F
Pd
N
H2

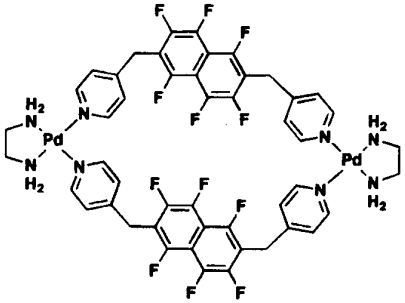
F
Pd
N
H2

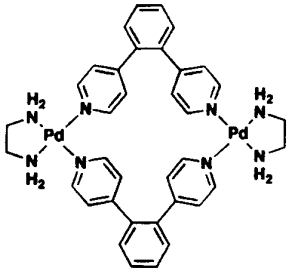
Pd
N
H2

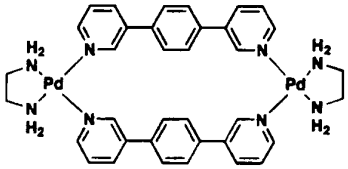
Pd
N
H2

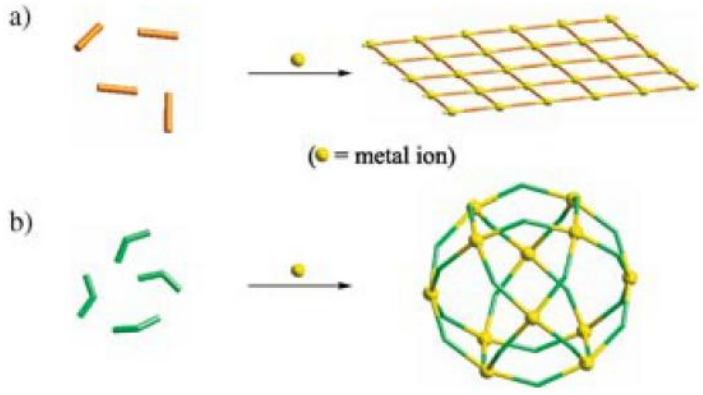
a)
(● = metal ion)
b)

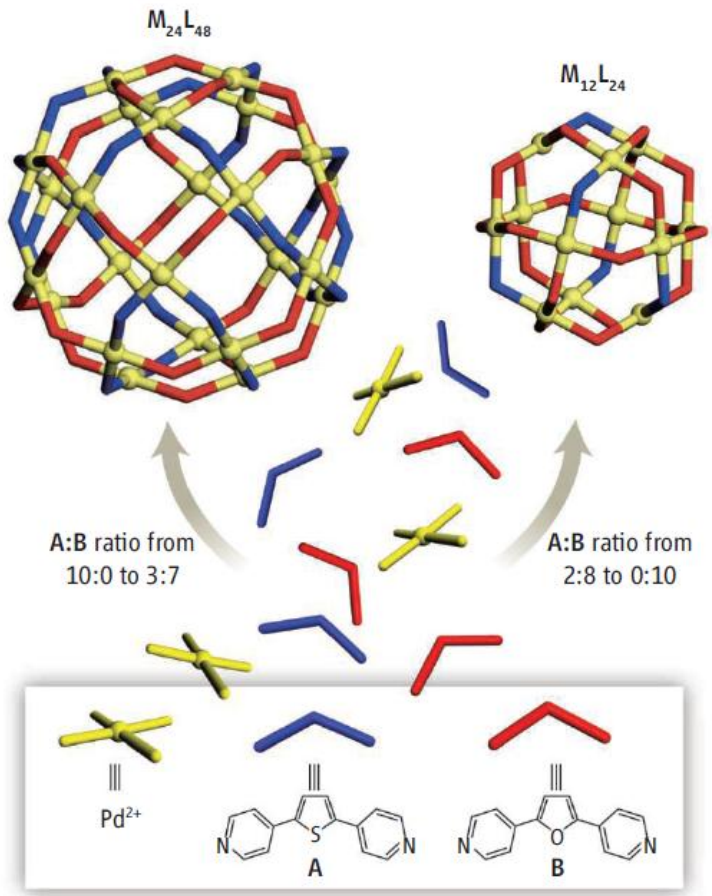
$M_{24}L_{48}$
$M_{12}L_{24}$
A:B ratio from
10:0 to 3:7
A:B ratio from
2:8 to 0:10
Pd^{2+}
A
B